

AD-A056 388

SRI INTERNATIONAL MENLO PARK CA  
ANALYSIS OF STRESS IONOGRAMS.(U)  
DEC 77 N J CHANG

F/G 4/1

UNCLASSIFIED

DNA-4486F

DNA001-77-C-0013  
NL

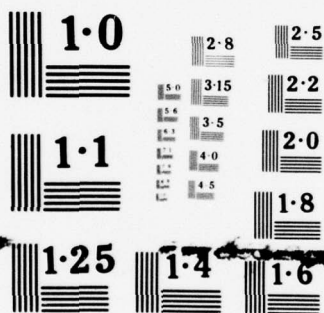
1 OF 1  
ADA  
056388



END  
DATE  
FILMED

8-78

DDC



NATIONAL BUREAU OF STANDARDS  
MICROCOPY RESOLUTION TEST CHART

**LEVEL II**

AD-E300 271  
12  
DNA 4486F

AD A 056388

## ANALYSIS OF STRESS IONOGRAMS

SRI International  
333 Ravenswood Avenue  
Menlo Park, California 94025

December 1977

Final Report for Period November 1976—October 1977

CONTRACT No. DNA 001-77-C-0013

APPROVED FOR PUBLIC RELEASE;  
DISTRIBUTION UNLIMITED.

THIS WORK SPONSORED BY THE DEFENSE NUCLEAR AGENCY  
UNDER RDT&E RMSS CODE B322077462 T25AAXHX63514 H2590D.

AJ NO.  
DDC FILE COPY

Prepared for

Director  
DEFENSE NUCLEAR AGENCY  
Washington, D. C. 20305

78 06 23 098

DDC

RECEIVED  
JUL 20 1978  
B

Destroy this report when it is no longer  
needed. Do not return to sender.





UNCLASSIFIED

SECURITY CLASSIFICATION OF THIS PAGE (When Data Entered)

REPORT DOCUMENTATION PAGE		READ INSTRUCTIONS BEFORE COMPLETING FORM
1. REPORT NUMBER DNA 4486F	2. GOVT ACCESSION NO.	3. RECIPIENT'S CATALOG NUMBER
4. TITLE (and Subtitle) ANALYSIS OF STRESS IONOGRAMS	5. TYPE OF REPORT & PERIOD COVERED Final Report, for Period November 1976 - October 1977	6. PERFORMING ORG. REPORT NUMBER SRI International Proj. 5908
7. AUTHOR(s) Norman J. F. Chang	8. CONTRACT OR GRANT NUMBER(s) DNA 001-77-C-0013	9. PROGRAM ELEMENT, PROJECT, TASK AREA & WORK UNIT NUMBERS Subtask T25AAXHX635-14
10. PERFORMING ORGANIZATION NAME AND ADDRESS SRI International 333 Ravenswood Avenue Menlo Park, California 94025	11. CONTROLLING OFFICE NAME AND ADDRESS Director Defense Nuclear Agency Washington, D.C. 20305	12. REPORT DATE December 1977
13. MONITORING AGENCY NAME & ADDRESS (if different from Controlling Office)	14. SECURITY CLASS (of this report) UNCLASSIFIED	15. NUMBER OF PAGES 64 P.
16. DISTRIBUTION STATEMENT (of this Report) Approved for public release; distribution unlimited.		
17. DISTRIBUTION STATEMENT (of the abstract entered in Block 20, if different from Report) (18) DNA, SPIE (19) 4486F, AD-E344 271		
18. SUPPLEMENTARY NOTES This work sponsored by the Defense Nuclear Agency under RDT&E RMSS Code B322077462 T25AAXHX63514 H2590D.		
19. KEY WORDS (Continue on reverse side if necessary and identify by block number) Ionograms                      Sporadic-E Radar Echoes                  Wind Shear Barium Echoes		
20. ABSTRACT (Continue on reverse side if necessary and identify by block number) Anomalous radar returns seen on ionograms following ionospheric barium releases are analyzed to determine their origin and their interpretation. Two types of echoes are identified; one type originates from the barium cloud and the other type from layers formed by the descent of barium ions into the E-region. A review is made of sporadic-E literature because some of the explanations of the origin and reflection mechanisms proposed for sporadic-E appear to be applicable to barium echoes. Data from past barium		

DD FORM 1473 1 JAN 73 EDITION OF 1 NOV 65 IS OBSOLETE

UNCLASSIFIED

SECURITY CLASSIFICATION OF THIS PAGE (When Data Entered)

410 281

next  
page  
hc

UNCLASSIFIED

SECURITY CLASSIFICATION OF THIS PAGE(When Data Entered)

20. ABSTRACT (Continued)

releases were also reviewed to supplement the STRESS data base. The findings indicate that reflection from an overdense layer or target is not the cause of the barium-associated returns. Thus, the maximum frequencies of the returns cannot be interpreted as a maximum plasma frequency. Gradient reflection and scatter from weak or strong irregularities are both plausible mechanisms for both types of echoes. The characteristics of the E-region returns and their likely cause (compression due to wind shear) suggest that these layers are thin with sharp boundaries and a rough underside.

UNCLASSIFIED

SECURITY CLASSIFICATION OF THIS PAGE(When Data Entered)

# CONTENTS

LIST OF ILLUSTRATIONS. . . . .	2
LIST OF TABLES . . . . .	3
I INTRODUCTION. . . . .	5
A. General. . . . .	5
B. Background . . . . .	5
II REVIEW OF MIDLATITUDE SPORADIC-E LITERATURE . . . . .	10
III ANALYSIS OF PRE-STRESS AND STRESS IONOGRAMS . . . . .	14
A. Nature of the Reflecting Layers. . . . .	16
1. Migration of Barium Ions to the Lower E-Region. . .	20
2. Interaction Between E- and F-Region Caused by Barium Releases . . . . .	23
B. Reflection of Radio Waves by Barium Ionization . . . . .	27
IV CONCLUSIONS . . . . .	32
REFERENCES . . . . .	34
APPENDICES	
A. IONOSPHERIC DATA . . . . .	37
B. MAGNETOMETER RESULTS . . . . .	59

ACCESSION for		
NTIS	White Section	<input checked="" type="checkbox"/>
DDC	Gray Section	<input type="checkbox"/>
UNANNOUNCED		<input type="checkbox"/>
JUSTIFICATION _____		
BY _____		
DISTRIBUTION/AVAILABILITY CODES		
Dist.	AVAIL. and/or	SPECIAL
A		

78 06 23 098

1

## ILLUSTRATIONS

1	Sequence of Ionograms for Event FERN Showing the Migration of the Reflection Layer from the F-Region to the Lower E-Region. . . . .	18
2	Range-Time History of Barium Echoes for Event FERN . . . . .	20
3	Altitude of Ion Cloud as a Function of Time--Event FERN. . .	21
4	Motion of Ion Cloud with 20-Minute Markers--Event FERN . . .	24
5	Schematic Picture Showing How an F-Region Barium Cloud Interacts with the Underlying E-Region Through the Equipotential Geomagnetic Field Lines. . . . .	25
A-1	f-Plot for Event ANNE. . . . .	40
A-2	f-Plot for Event BETTY . . . . .	41
A-3	f-Plot for Event CAROLYN . . . . .	42
A-4	f-Plot for Event DIANNE. . . . .	43
A-5	f-Plot for Event ESTHER. . . . .	44
A-6	f-Plot for Event FERN. . . . .	45
A-7	Ionograms Taken on 1 and 2 December 1976 for Event ANNE. . .	46
A-8	Ionograms Taken on 2 and 3 March 1977 for Event CAROLYN. . .	48
A-9	Ionograms Taken on 8 and 9 March 1977 for Event DIANNE . . .	49
A-10	Ionograms Taken on 13 and 14 March 1977 for Event ESTHER . .	50
A-11	Ionograms Taken on 14 and 15 March 1977 for Event FERN . . .	52
B-1	Magnetic Index for Eglin, Florida Derived from EDA Fluxgate Magnetometer During The STRESS Program. . . . .	61

## TABLES

1	Summary of Barium Signatures Seen on Pre-STRESS and STRESS Ionograms . . . . .	8
A-1	Summary of Pre-STRESS and STRESS Releases. . . . .	39



## I INTRODUCTION

### A. General

This report describes the results obtained from operation of an ionosonde during the Pre-STRESS and STRESS experiments conducted at Eglin, Florida during the winter and spring of 1976/1977. The analysis is directed at interpretation of anomalous returns seen on ionograms obtained after each barium release. These returns are shown to originate from the barium ion cloud and from layers created from barium ions migrating to the E-region.

The nature of radio waves reflected or scattered from barium layers is examined in light of sporadic-E theories and experimental results. In addition, mechanisms proposed for the generation of sporadic-E layers are assessed to determine their applicability to barium layers.

### B. Background

On 1 December 1976 and during February and March 1977, six ionospheric barium releases were made, each on one of six late afternoons or evenings near Eglin AFB, Florida. The releases were made for the purpose of generating a region of structured ionization that would occlude transmissions between an aircraft and a synchronous satellite. These experiments, sponsored by the Defense Nuclear Agency (DNA) in cooperation with the Air Force Electronics System Division (ESD) and the Air Force Avionics Laboratory (AFAL), were conducted to evaluate satellite communication links under conditions that simulate many aspects of a post-nuclear-burst environment.

An integral part of the experiment was the FPS-85 radar operating in an incoherent-scatter mode. This instrument was tasked to track the ion cloud (in order to properly position the aircraft with respect to the satellite and ion cloud) and to provide diagnostic information on electron densities within the cloud.

In support of the FPS-85 radar, SRI operated a vertichirp ionosonde to provide  $f_oF_2$  measurements for calibration of the FPS-85 radar. Additional objectives of the vertichirp radar were to obtain electron density profiles of the background ionosphere (used to calculate ambient Pedersen conductivities for the six barium releases), and to serve as a real-time monitor of the state of the ionosphere. Unfortunately, virtually no ionospheric data were obtained below 200 km, so it has not been possible to calculate the desired conductivities.

It is not known why ionospheric returns, which would normally originate from the E-region in the late afternoon or evening, are absent below 200 km. However, a number of possible reasons can be cited: (1) In the evenings the noise background was fairly high between the lower-frequency limit of the sounder and about 1 or 2 MHz, thus obscuring any ionospheric returns that might have existed in this frequency range; (2) although the lower-frequency limit of the vertichirp was 0.5 MHz, on most inograms the actual limit appeared to be about 2 MHz; (3) the sensitivity of the vertichirp at low frequencies was poor; and/or (4) E-layer critical frequencies were below the lower limit of the system.

This lack of ionospheric returns below 200 km also occurred during SECEDE II and HAPREX, which required assuming a density model for that region in order to generate Pedersen conductivities. This exercise was not repeated here because actual E-region data can be obtained from the FPS-85 radar or the rocket probe measurements. In addition, since the conjugate ionosphere is believed to play at least as important a role in cloud dynamics as does the sunlit ionosphere, it made little sense to calculate conductivities from an E-region model when no conjugate measurements were made.

In terms of its primary objective--obtaining  $f_oF_2$  values for the FPS-85 radar--the vertichirp operated successfully on all six Pre-STRESS and STRESS releases. On BETTY equipmental problems caused a loss of data shortly after release (0002 UT) until the problem was corrected at 0100 UT). Good data, however, were obtained prior to the vertichirp outage and after 0100 UT.

1

A somewhat unexpected bonus of the vertichirp operation was the observation of intense and persistent E- and F-region returns that are believed to originate from the barium ion cloud because of their occurrence in approximately the same time and range space as the cloud. Table 1 summarizes the barium signatures seen on the Pre-STRESS and STRESS ionograms. Intense E- and F-region echoes were observed on Event FERN. The E-region echoes were particularly strong, indicating returns from frequencies as high as 18 MHz. For the other three releases (CAROLYN, DIANNE, and ESTHER) weak F-region traces lasting several minutes were observed. No barium-associated echoes were observed for Event BETTY because of an untimely equipment failure during the period when returns from the barium cloud would have occurred. When the vertichirp resumed operation at R + 68 min, a weak sporadic layer was observed between 2 and 4 MHz. Although the association of this trace with the barium cloud cannot be ruled out, we believe that this signature was not related to the barium cloud because ionograms on several non-release days had similar echoes at similar times. We feel, however, that had the vertichirp been operational throughout the times of interest, F-region returns from BETTY would have been observed.

Although barium echoes were also observed during other barium release series (SECEDE II and III), the STRESS results were particularly interesting for the following reasons: (1) The returns for FERN showed a clear downward migration of the reflecting layer, thus implying that Ba ions moved down to the lower E-region; and (2) the maximum frequency of the E-region returns for FERN was 18 MHz at R + 81 min. The significance of these results is not clear since it is difficult to accept critical frequencies this large at late times.

Previous reports of barium-associated returns on ionograms (Oetzel and Chang, 1969; Simons, 1971a, 1971b; Baender, 1971; Chang, 1971)\* for the most part described the observations but made no attempt to explain the nature of the reflecting layers or the significance of the returns.

---

\*References are listed at the end of this report.



Table 1  
SUMMARY OF BARIUM SIGNATURES SEEN ON  
PRE-STRESS AND STRESS IONOGRAMS

Event	First Ba Echo	Last Ba Echo	Duration (min)	Maximum Frequency (MHz)	Remarks
ANNE	R + 13.7 min (2324 UT)	R + 97.7 min (0048 UT)	84	15	Strong, continuous F-region echoes
BETTY	No data	No data	No data	No data	
CAROLYN	R + 17.8 min (0012 UT)	R + 29.8 min (0024 UT)	12	10	Weak F-region echoes
DIANNE	R + 44.9 min (0046 UT)	R + 72.9 min (0114 UT)	28	9	Weak F-region echoes
ESTHER	R + 17.8 min (2319 UT)	R + 20.8 min (2322 UT)	3	10	Weak F-region echoes
FERN	R + 12.8 min (2259 UT)	R + 213.8 min (0220 UT)	201	18	Strong, continuous E- and F-region echoes

Thus, the questions raised concerning the nature of the reflecting layers (image or Ba ions) and the interpretation of the critical frequencies have not hitherto been addressed.

This report will be concerned primarily with the interpretation of the barium-related returns seen on the ionograms. Of particular interest are the interpretation of the barium returns in terms of peak densities, the origin of the apparent barium-cloud-related sporadic-E echoes, and the possible interaction of the barium cloud with underlying layers. Since the barium returns bear such a close resemblance to sporadic-E returns, a review of the literature (Section II) was conducted to determine the relevance of previous work to the present study. It was found that the mechanism believed responsible for midlatitude sporadic-E (compression of metallic ions by horizontal wind shears) plays a major role in creating the reflecting Es layers seen on the ionograms. Furthermore, wind shear may have played a role in Event FERN. In addition, the nature of sporadic-E reflection of radio waves appears to be applicable to the Ba traces. These results will be discussed in Section III, with the conclusions following in Section IV.

To permit ready access to the ionospheric and magnetic data that were collected during the STRESS program, f-plots and ionograms for each of the releases are presented in Appendix A. Appendix B contains a brief discussion of the magnetometer operation and a summary of the results.

## II REVIEW OF MIDLATITUDE SPORADIC-E LITATURE

Sporadic-E is a term used to describe a distinctive trace on ionograms in the 90-to-120-km height regime. At midlatitude these traces, characterized by a relatively height-independent echo of a transient nature, are normally quite distinct from the E-region returns. At times the maximum frequency returned from sporadic-E layers can be much greater than the returns from any of the other layers. Sometimes the sporadic-E layer is opaque and partially or completely blankets anything above it. On other occasions the upper layers appear to be unaffected by the underlying sporadic-E layer. Retardation near the maximum frequency of the Es trace is sometimes present, implying that the layer is relatively thick with a well defined peak electron density. On other occasions the trace is narrow and shows no retardation, suggesting reflection from a thin layer or from a sharp boundary. Sometimes magnetoionic splitting at the low-frequency end of the trace may be visible; usually there is none.

Attention herein is primarily directed at midlatitude sporadic-E because both its origin and reflection mechanism potentially apply to the interpretation of barium echoes. Two other categories of sporadic-E exist--auroral and equatorial. However, the physical phenomena generally associated with these--auroral particle precipitation and scattering by plasma waves in the electrojet, respectively--do not appear to be germane to this discussion. These two types will not be considered here.

Sporadic-E has been a popular topic of research for many years, and hundreds of theoretical and experimental papers and reports currently exist. There have been numerous seminars and conferences on the subject, and three have led to special issues of Radio Science (March 1975; March 1972); February 1966) being devoted to the papers presented. These issues, as well as a book edited by Smith and Matsushita (1962), a review by Whitehead (1970), and most recently a comprehensive report by Miller and Smith (1976) serve as an ideal starting point for the uninitiated reader.

The number of different explanations and theories on the origin, generation mechanism, and scattering mechanism responsible for Es indicates the complexity of the subject. In spite of all this interest, however, many features of sporadic-E layers remain unexplained. It has only been within the last ten years that a theory regarding the origin of midlatitude sporadic-E layers has gained general acceptance. This is the wind-shear theory originally proposed by Dungey (1956; 1959) and developed by Whitehead (1961), Axford (1963), and MacLeod (1966). The theory is consistent with many of the observed features of Es and is now believed to explain at least some of the observed Es traces.

The wind-shear model contends that long-lived metallic ions from ablating meteors are compressed into thin layers by the combined action of the horizontal neutral wind and the geomagnetic field. Specifically, in the lower E-region, where the ion-neutral collision frequency exceeds the ion gyrofrequency, the ions are effectively moved by the neutral particles. As the ions move they are subject to a Lorentz force that acts perpendicular to both the predominantly horizontal neutral wind and the geomagnetic field. Thus, the ions can acquire a significant vertical component of motion while the electrons are dragged along by the polarization fields. Often large vertical shears exist in the neutral wind and these in turn lead to vertical shear of the ion motion. The resulting convergence and divergence of the ion flow can produce a net flow of ionization into a region and thus cause an enhancement of ion density. (Correspondingly, however, when there is a net flow out of the region there is a depletion of ion density.) Because metallic ions have a long lifetime in the lower E-region, the density of the enhanced layers will increase (or decrease) with time.

Other mechanisms--instability and turbulence--have been suggested as an alternative to the wind-shear theory, but these do not appear as applicable to midlatitude sporadic-E. Also, in terms of application to barium-associated E-region returns, the wind-shear theory appears the most attractive and will be discussed in Section III.

Since ionograms probably provide the bulk of sporadic-E observations, much effort has been directed toward providing an explanation of these

signatures. The interpretation of two parameters-- $f_b Es$  and  $f_t Es$ --that are used to describe the appearance of sporadic-E echoes on ionograms, is of particular interest. The first term ( $f_b Es$ , the blanketing frequency) is used to specify the frequency of a partially transparent sporadic-E layer, above which the upper layers are visible and below which the upper layers are obscured. The second term ( $f_t Es$ , the top frequency or sometimes the critical frequency) specifies the highest frequency returned from the layer.

These parameters can be related to peak densities in the layer if certain assumptions regarding the reflection medium are made. Two models have been proposed (Reddy, 1968):

- (1) Thin-layer model, in which gradient reflection from thin horizontally stratified layers is responsible for the Es trace.
- (2) Patchy-layer model, in which reflection or scatter from irregularities embedded in the layer are responsible for the Es returns.

Each of these models and variations of them have been tested against observations, and each is capable of explaining certain features of Es.

The thin-layer model attributes reflection to the large electron-density gradients that characterize the vertical profile of Es layers revealed by rocket flights. Reflection coefficients, calculated from a full-wave solution of the wave equation, indicate that gradient reflection can produce Es returns of sufficient strength to be seen on the typical ionogram (Reddy, 1968). Miller and Smith (1976) found, however, that the range of partial transparency observed (difference between  $f_b Es$  and  $f_t Es$ ) cannot be explained by gradient reflection from the profile associated with the particular sporadic-E layer.

The patchy-layer model features dense blobs of ionization embedded in a background of lower electron concentration. The peak density of these blobs correspond to  $f_t Es$ , the maximum frequency of the sporadic-E reflection, and therefore signals incident on them with frequencies below this value are totally reflected. The blanketing frequency,  $f_b Es$ , on the other hand, corresponds to the minimum uniform electron density in the



background. Radio waves with frequencies exceeding this value are able to penetrate the layer and be reflected from a higher layer.

A variation of the patchy-layer model envisions small-scale irregularities in the vertical electron density distribution. Energy is returned from these layers as described by the scattering theory of Booker and Gordon (1950), and Gordon (1958).

While there are sufficient theories and observations of sporadic-E against which to test these models, existing observations of barium echoes are not of sufficient quality to permit similar comparisons. Nevertheless the wind-shear theory and the reflection models discussed above can be used in Section III to aid in the interpretation of the data.

### III ANALYSIS OF PRE-STRESS AND STRESS IONOGRAMS

Observation of traces on ionograms that appear to be associated with barium releases is not new. Such effects were probably first recorded by investigators from the Max-Planck Institute in the late sixties (Rieger et al., 1968). Similar effects were also reported during SECEDE II and III, and more recently in the STRESS program.

During SECEDE III, conducted in Alaska during March 1969, nine barium releases of various yields were made, ranging from 2.4 kg to 96 kg. Although two Ba canisters were released at different heights on each of the first three days of the test series, these multiple releases will be counted as a single event. Thus, there were six events.

Ionograms taken at College, Alaska showed traces that are attributable to reflection or scatter from the ion cloud for three of the six events. These traces, for the most part, occurred at a virtual height of 200 km, in agreement with the slant range to the cloud from the ionosonde. The echoes lasted a few minutes and were first observed roughly ten minutes after release. In addition, the frequency extent of the echoes was typically less than 1 Hz except for the large 96-kg release, which had a frequency extent from 4 to 8.5 MHz.

Three of the events apparently did not produce any noticeable echoes on ionograms, but propagation conditions or the yield of the release were judged responsible (Oetzel and Chang, 1969; Chang, 1971).

During SECEDE II, conducted in Florida in 1971, six 48-kg barium releases were made. Each of these produced clear ionospheric effects and in fact on three releases the resulting E-layer was sufficiently dense that the upper layers were blanketed. Since  $f_oF_2$  at the time of blanketing was in the 4-to-5-MHz range, a lower estimate of the peak electron concentration in the cloud  $2 \times 10^{11}$  el/m<sup>3</sup>. The onset of blanketing occurred typically about 100 minutes or more after the release, and the duration was a few tens of minutes.

With the exception of the times when the F-region was blanketed by the underlying Eb-layer, SECEDE II ionograms showing returns from the barium cloud are quite similar.\* In general, they have the following characteristics: (1) The onset of barium echoes occurred about 2 to 10 minutes after release; (2) mixed-mode echoes<sup>†</sup> were generally the first evidence of the barium cloud; (3) multiple echoes separated by 10-to-20 km were typical as the trace developed; (4) Eb or Fb traces<sup>‡</sup> were generally very thin, but on occasion they were as much as 50 km thick; (5) retardation or magnetoionic splitting was not observed; (6) partial blanketing of the upper layers was not evident on the ionograms inspected even prior to and following the passage of the blanketing layer, thus suggesting a layer of limited horizontal extent; (7) ionograms for OLIVE showed the virtual range decreasing at a rate of about 14 m/s. This value was consistent with radar measurements at 10 MHz, which indicated a descent of 17 m/s during the first hour.

Although not as striking as the SECEDE results, the STRESS ionograms exhibit approximately the same behavior as summarized above, with the following exceptions: (1) There is a hint of magnetoionic splitting near 6 MHz, and a hint of retardation at the high-frequency end of the F-region trace in ANNE at 2338 UT; (2) the first evidence of the barium echo generally occurred later (in the 10-to-20-minute time frame) than in SECEDE; and (3) blanketing of the upper layers was not observed for any of the releases.

---

\* These conclusions were based on inspection of available SECEDE II ionograms published in reports. The results, however, pertain primarily to OLIVE, since this is the only event for which a complete set of ionograms was available.

<sup>†</sup> Mixed-mode echoes identify returns from a propagation path that includes some combination of traverses between the ion cloud, the ionosphere, and the ionosonde. This indirect route leads to a longer path and thus this type of returns can be distinguished from the direct path between the ion cloud and the ionosonde.

<sup>‡</sup> For brevity, barium-associated traces on ionograms will be designated as Fb or Eb if they occur at F- or E-region heights, respectively.



Figure 1 illustrates some of the salient features that are discussed in this section. This figure shows ionograms taken shortly after the FERN release and during a particularly interesting period when the F-region trace developed and subsequently moved down to the lower E-region. FERN was released at 2246:09 UT, with apparently no effect evident on ionograms taken at 2247 and 2250 UT. The first evidence of the barium release occurred at 2253. At this time a faint trace appeared below the F-layer trace at about 4 MHz. The intensity and frequency extent of this trace increased in each subsequent ionogram and by 2309, or R + 23 min, it was clearly visible. At this time the trace developed a "nose" at the low-frequency end and showed a slight amount of frequency dependence at each end of the return.

The minimum virtual height of the Fb trace at 2309 was 185 km. In the next sequence of seven ionograms, covering a time period of 23 min, this trace decreased in intensity and frequency extent while descending to 130 km. At 2332 the Eb returns occurred primarily between 2 and 4 MHz, but near 8 MHz there was a hint of Fb returns at a height of 200 km.

Starting from 2335 the Eb trace continued to descend, but its frequency extent increased until at 0007 UT the maximum frequency returned was 18 MHz. The layer reached a minimum altitude of about 105 km at 0025 UT, and after this time the minimum height of reflection started to increase with time such that by 0203 UT it was at a height of 135 km.

The above scenario suggests a number of important questions: (1) What significance can be attached to the maximum frequency returned from the Eb or Fb layers? (2) What is the nature or origin of the reflecting layers? (3) What is the reflection or scattering mechanism? (4) What is the cause of the echo intensity variation with time? These questions will be addressed in the remainder of this section.

#### A. Nature of the Reflection Layers

The contention that F-region traces of the type depicted in Figure 1 result from the barium ion cloud rests on the assumption that these traces originate in a time and range space similar to that of the ion cloud, and

upon the uniqueness of these returns. That is, these signatures are not normal ionospheric returns, and were never observed on non-release days.

In FERN the downward migration of the reflecting layer from a virtual height\* of 200 km to 115 km over a 60-min period is taken as evidence that barium ions do descend to the lower E-region and are the cause of the Eb-returns.† The possibility of barium ions descending to the lower E-region and forming layers that reflect incident radio signals has been suggested in the past (Thome, 1971; Mende, 1971a). The opinions of these authors were based primarily on ionograms and HF radar data indicating that typically the reflecting layer approached the observer, reached a minimum range, and then receded from the observer. While a descending Ba layer that reaches a minimum height of approximately 110 km and subsequently passes away from the observer would be consistent with observations, an equally plausible model is that the returns are due to reflection from an E-layer enhancement induced by the F-region cloud. Motion of this enhancement overhead would be consistent with the range-time history observed.

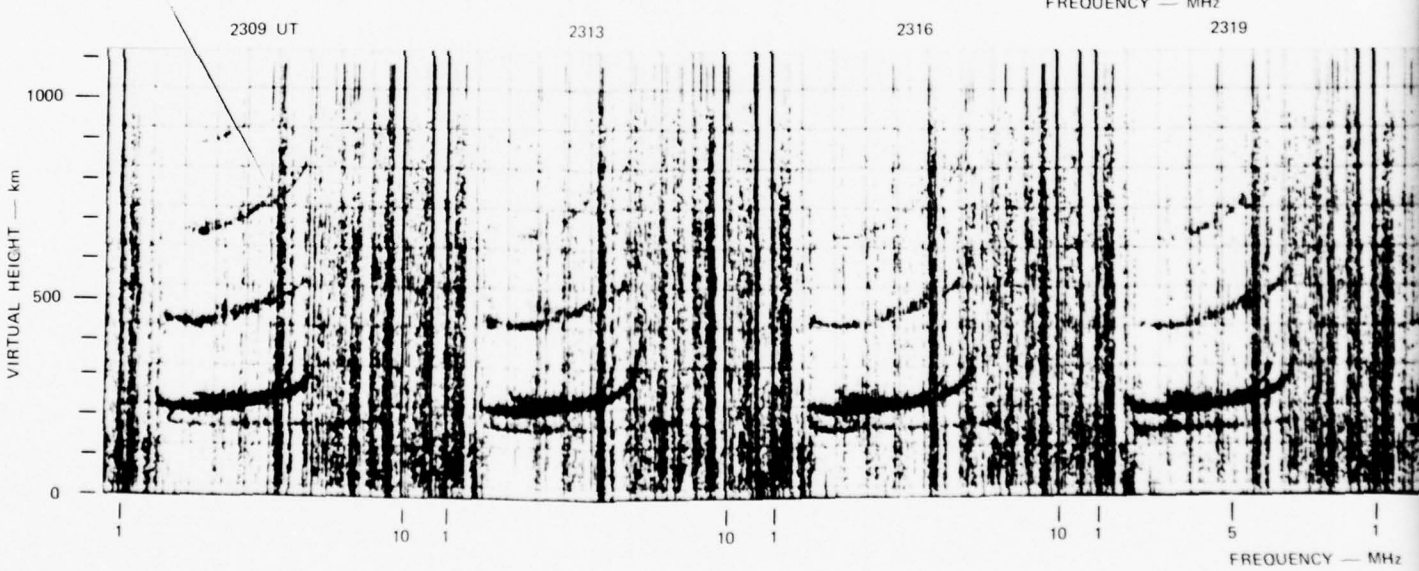
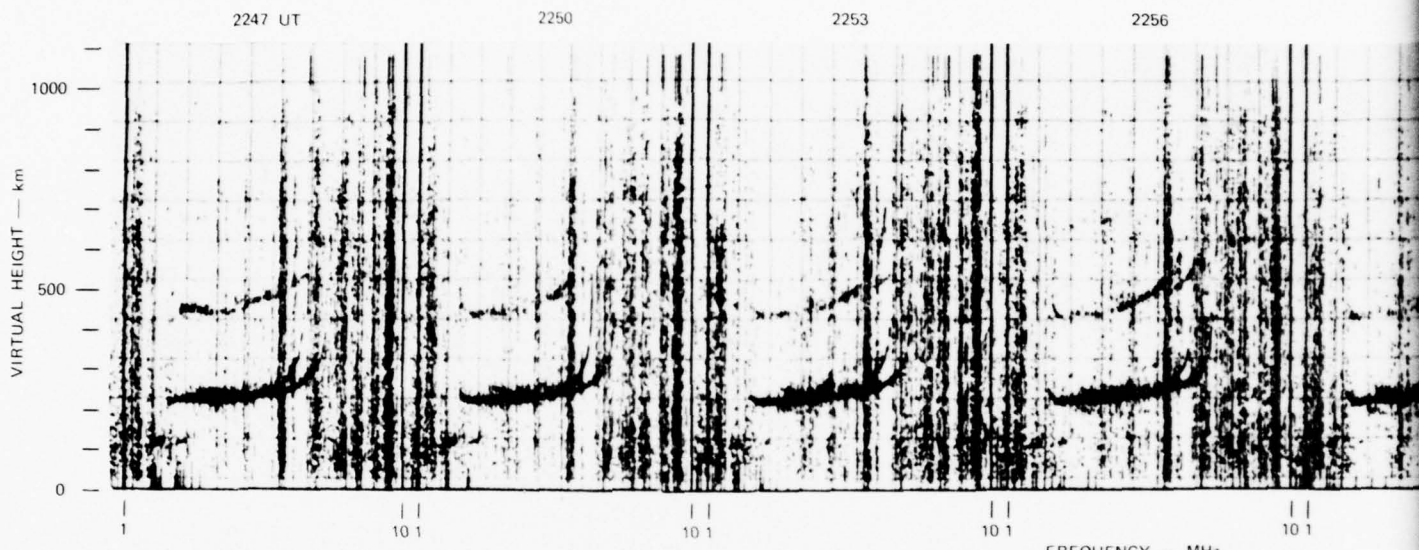
A firm position on these two models was not taken during the SECEDE program, apparently because arguments could be made in favor of either one. We feel, however, that the FERN ionograms show conclusively that barium ions do descend to the lower E-region and are the cause of the Es return. This conclusion is further supported by the FPS-85 radar measurements and by the SECEDE II data.

Furthermore, the development of the echo as the layer descends suggests that the ions are compressed into thin layers, with a corresponding increase in cross section. Such behavior is consistent with that predicted

---

\*The virtual-height label used on ionograms is correct only for a vertical propagation path. For off-vertical paths the term range or group path should be used. Our use of the term is only in reference to the label on the ionograms and does not imply any specific propagation path.

†The cause of radio-wave reflection is actually the electrons that are dragged along by the polarization fields.



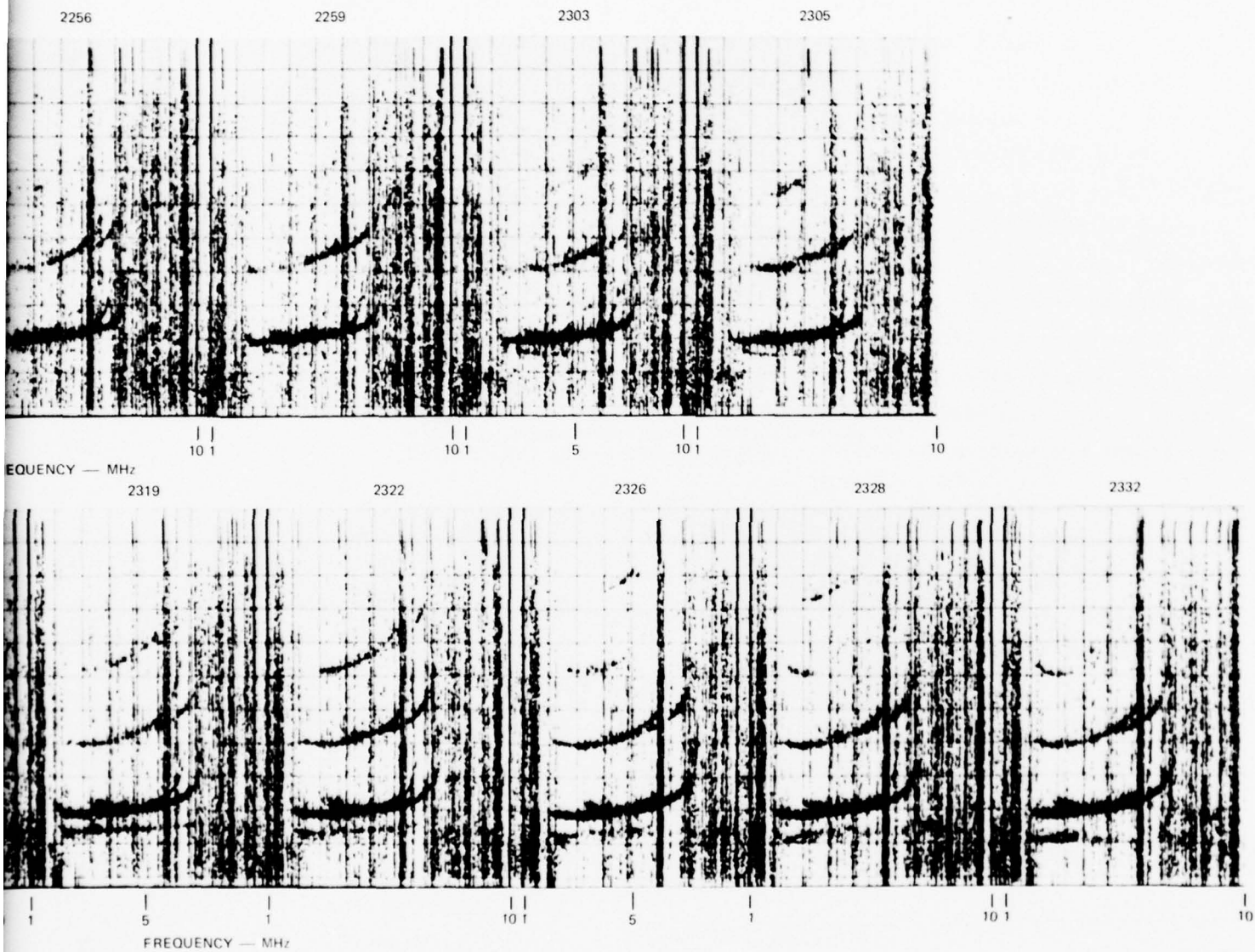


FIGURE 1 SEQUENCE OF IONOGRAMS FOR EVENT FERN SHOWING THE MIGRATION OF THE REFLECTION LAYER FROM THE F-REGION TO THE LOWER E-REGION



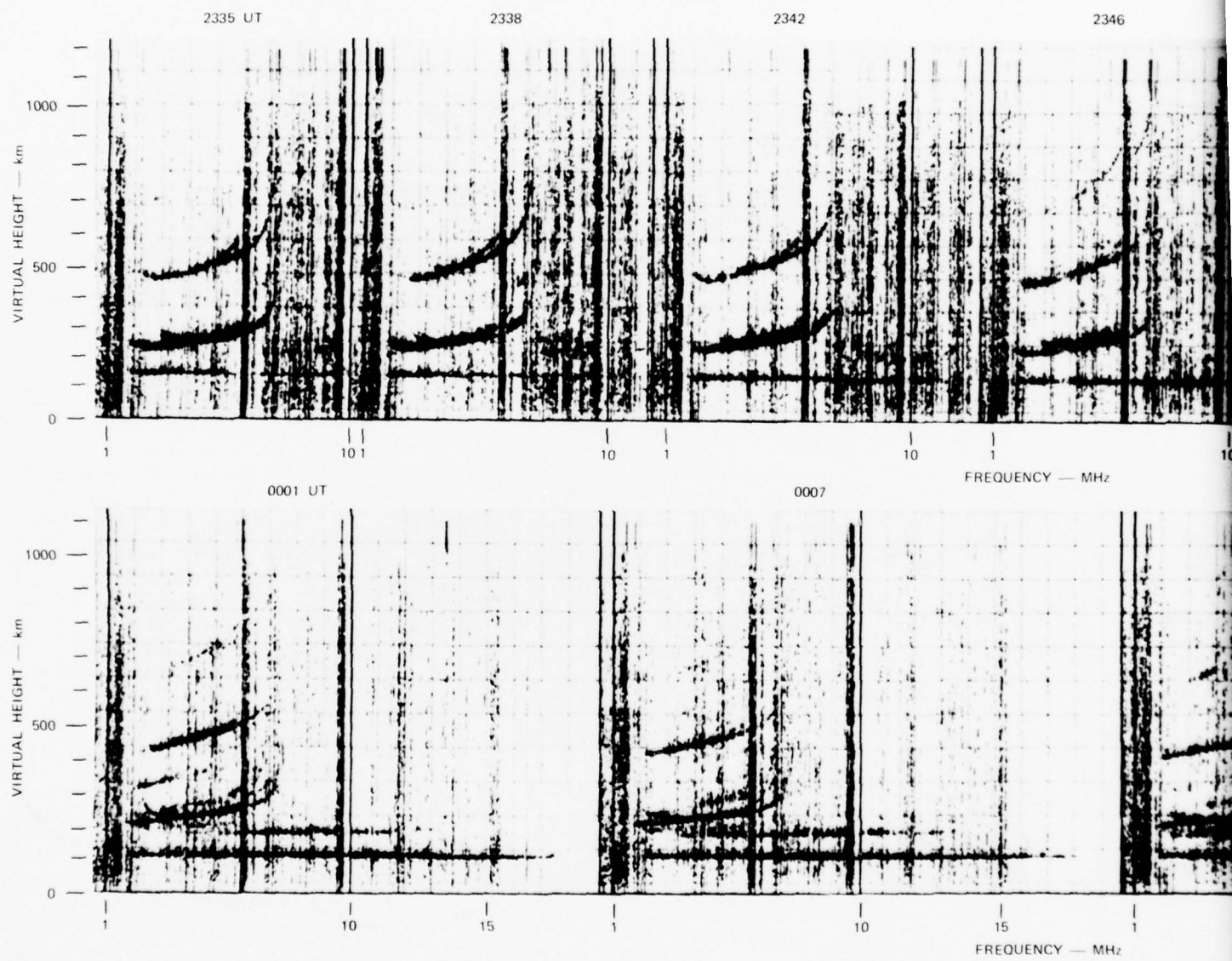
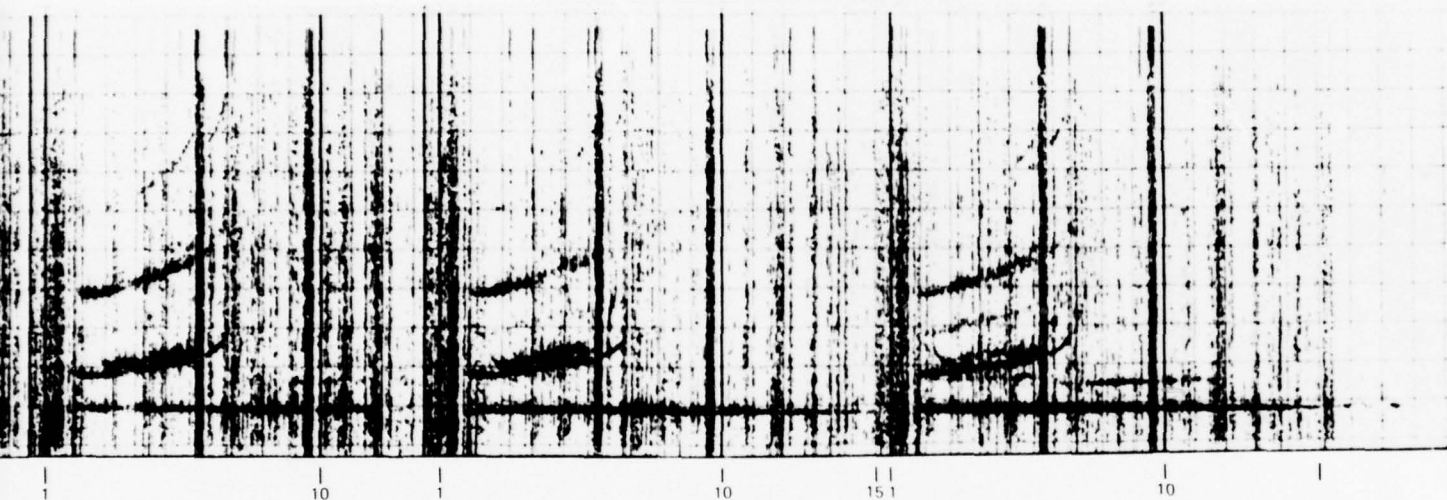


FIGURE 1 (Concluded)

2346

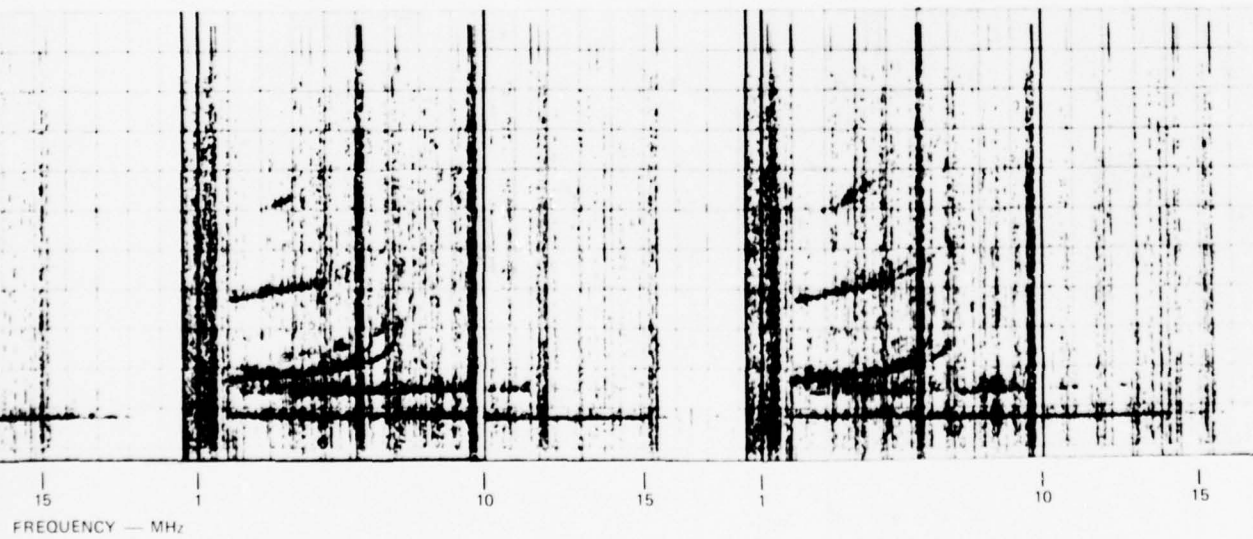
2350

2355



0014

0020



FREQUENCY — MHz

by wind-shear theory. Thus, the Eb trace in FERN is a graphic example of how a sporadic-E layer is created by the compression of metallic ions, and gives support to wind shear as the probable mechanism of Eb returns or Sporadic-E.

# 1. Migration of Barium Ions to the Lower E-Region

Figure 2 shows the range-time history of barium echoes observed during FERN. This figure shows that the barium cloud, released at an initial range of 221 km from the ionosonde, separated into two parts that drifted toward the observer at different rates. One part, which we shall designate the secondary cloud, approached the radar at about 24 m/s during the first 60 min, reached a minimum range of 105 km at R + 104 min, and then receded at about 11 m/s.

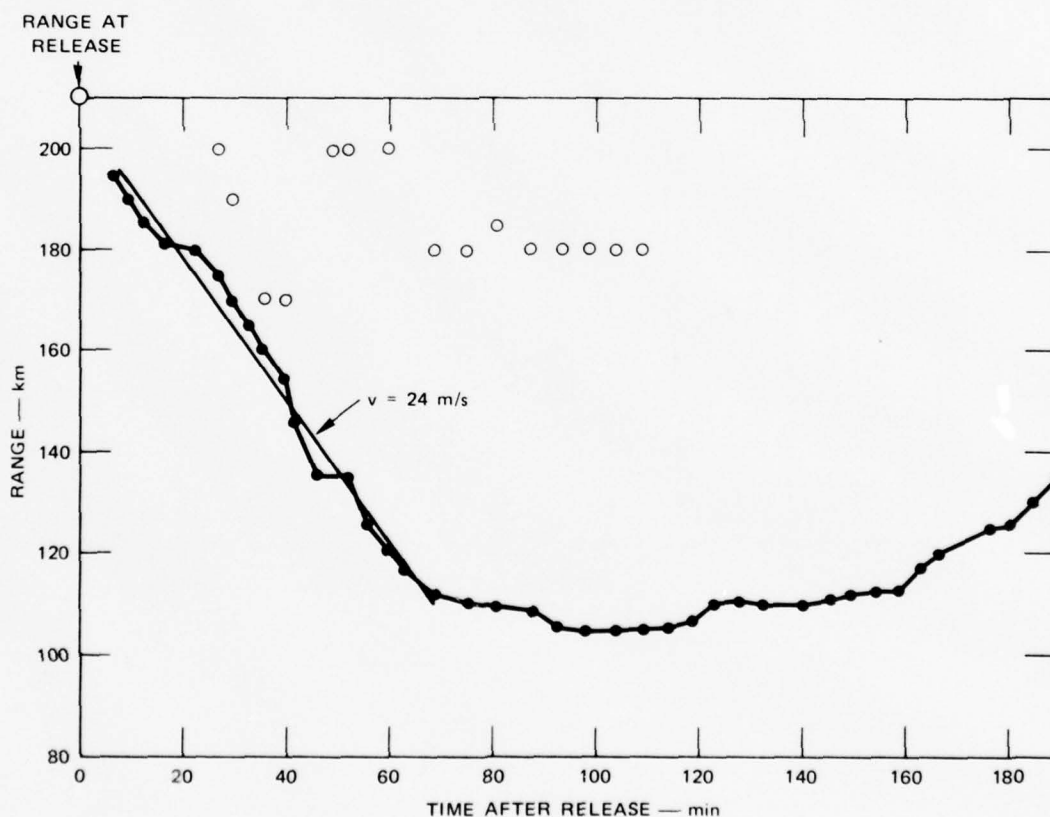


FIGURE 2 RANGE-TIME HISTORY OF BARIUM ECHOES FOR EVENT FERN

The quality of the Fb returns was poor during the first 60 min and considerable scatter can be seen in these range points. After R + 60 min, however, the Fb trace became quite distinct (see Figure 1), so greater confidence can be placed in these points. Because of the scatter the early behavior of the layer causing the Fb returns is uncertain, but based on the known range of the cloud at release (221 km) and the range of the layer after R + 60 min it is clear that this part of the cloud also approached the ionosonde, but at a slower rate.

The descent of a portion of the FERN ion cloud into the E-region is also supported by the FPS-85 measurements shown in Figure 3. During the first 60 min the radar tracked a portion that began near the release height and fell to 143 km. At approximately R + 55 min the radar switched to another part (we shall call this the main cloud, since it is this cloud that later became visible), which at that time had descended to 172 km.

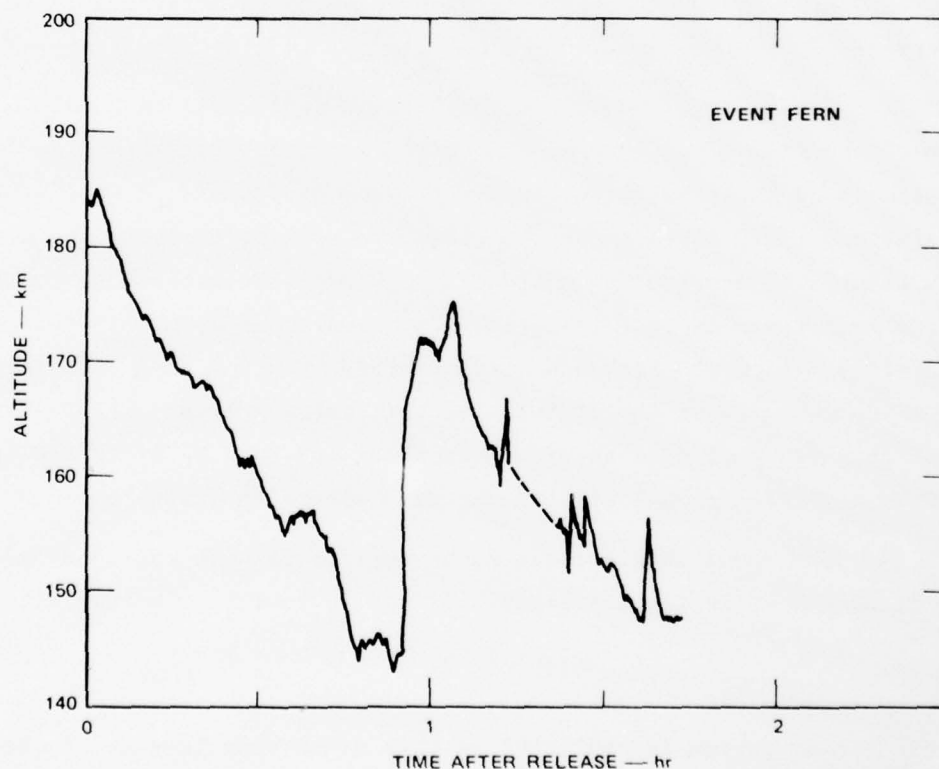


FIGURE 3 ALTITUDE OF ION CLOUD AS A FUNCTION OF TIME — EVENT FERN



If we assume a uniform rate of descent for this target we find that its descent rate over the first 60 min is about 4 m/s, compared to 12 m/s for the secondary cloud. After  $R + 60$  min, however, the main cloud also showed a rapid descent until  $R + 100$  min, when the radar was no longer able to track the cloud.

Before proposing a model that appears to be consistent with the vertichirp and FPS-85 data, let us digress and consider how ions move in a magnetic field. Above about 130 km, and especially so at greater altitudes, collisions between barium ions are infrequent compared to the ion gyrofrequency. Hence, to first-order, barium ions can freely move only in the direction of the magnetic field. When barium ions are released in sunlight at 185 km they quickly become ionized, forming a spherical cloud. This initial shape is distorted by gravity, the ambient electric field, and/or by the neutral winds.\* Because of the magnetic-field constraint, only a northward component of the neutral wind, a westward component of the electric field, or gravity is effective in causing a vertical motion of the barium ions.

Since it is known from optical and radar data that only a portion of the FERN cloud descended into the E-region, the mechanism driving the ion cloud down the field lines must also be capable of causing this separation. This division of the cloud can only be explained by a vertical wind shear. If gravity is neglected, the observed vertical motion of 12 m/s requires a neutral wind with a northward component of at least  $12/\sin(60) = 14$  m/s. Although winds of this magnitude and even larger are known to exist at the altitude of the barium release, little is known about the nature of wind shears above about 160 km. We offer the behavior of FERN as evidence that significant wind shears do exist above 180 km.

The model that appears to be consistent with the ionosonde and FPS-85 measurements discussed above is the following: Shortly after

---

\* Ambipolar diffusion is neglected in this discussion because it occurs roughly equally in both directions parallel to the magnetic field. Hence, to first order, it does not displace the cloud, taken as a whole.

release, wind shear caused the lower portion of the ion cloud to separate from the main cloud. Both clouds drifted eastward at about 23 m/s due to an ambient  $E \times B$  force (see Figure 4). The upper part of the ion cloud (main cloud), which was unaffected by the neutral wind, had an additional downward motion due to gravity. This descent rate, given by the ratio of the acceleration of gravity to the barium-ion collision frequency, is about 6 m/s at 180 km, a value consistent with the implied descent rate of 4 m/s in Figure 3. The lower part, however, descended at a faster rate--12 m/s--because of gravity plus an additional contribution due to a northward component of the neutral wind.

A common eastward motion due to  $E \times B$  was postulated for both clouds because it is known that the ambient electric field does not vary with height. Figure 3, however, indicates that the secondary cloud shows an additional northward motion while the main cloud shows a southward motion. The resulting horizontal component toward the ionosonde plus the vertical motion indicated by Figure 2 for the secondary cloud is consistent with the 24-m/s range rate shown by Figure 2.

The main cloud appeared at a constant range from the ionosonde after  $R + 70$  min because its northward motion due to the descent of the ions down the field lines is compensated for by the southward motion of the cloud due to  $E \times B$  forces (see Figure 3). Apparently, as the main cloud slowly descended, primarily due to gravity, it encountered a strong northward neutral wind, which cause the descent rate shown in Figure 3.

## 2. Interaction Between E- and F-Region Caused by Barium Releases

The interaction of an F-region barium cloud with the underlying E-region was pointed out by Haerendel, Lust, and Rieger (1967). These investigators proposed that at F-region heights an ion cloud driven by an ambient electric field will become polarized because of charge separation arising from the difference in mobility between electrons and ions. This polarization field will in turn be neutralized by current flow along the equipotential magnetic field lines. These currents are carried by electrons due to their higher mobility along the field lines, while down

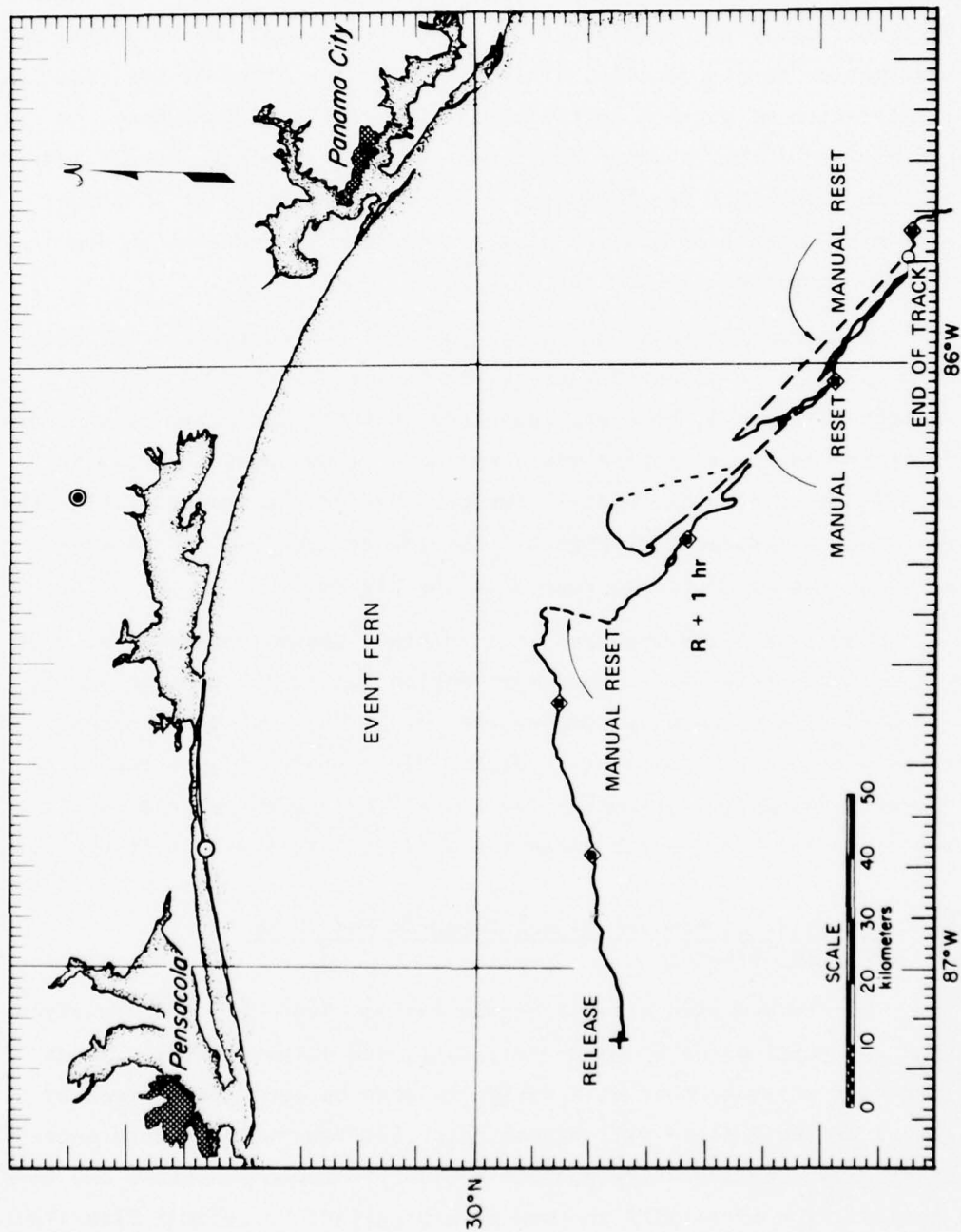


FIGURE 4 MOTION OF ION CLOUD WITH 20-MINUTE MARKERS — EVENT FERN

in the E-region, due to high Pedersen conductivity of the ions, the horizontal currents are largely carried by the ions.

The situation in the F-region, depicted in Figure 5, is that as the ions move away from the electrons in the barium cloud the polarization field created is neutralized by electrons arriving from the underlying E-region. The electrons, on the other hand, at the rear of the cloud flow down the field lines and tend to cause a local increase in electron density there. Below the front of the cloud there is a local increase of positive charges.

Experimental verification of the E-region interaction of ionospheric barium releases has been attempted with some success by Stoffregen (1970), although his efforts were somewhat inconclusive due to the

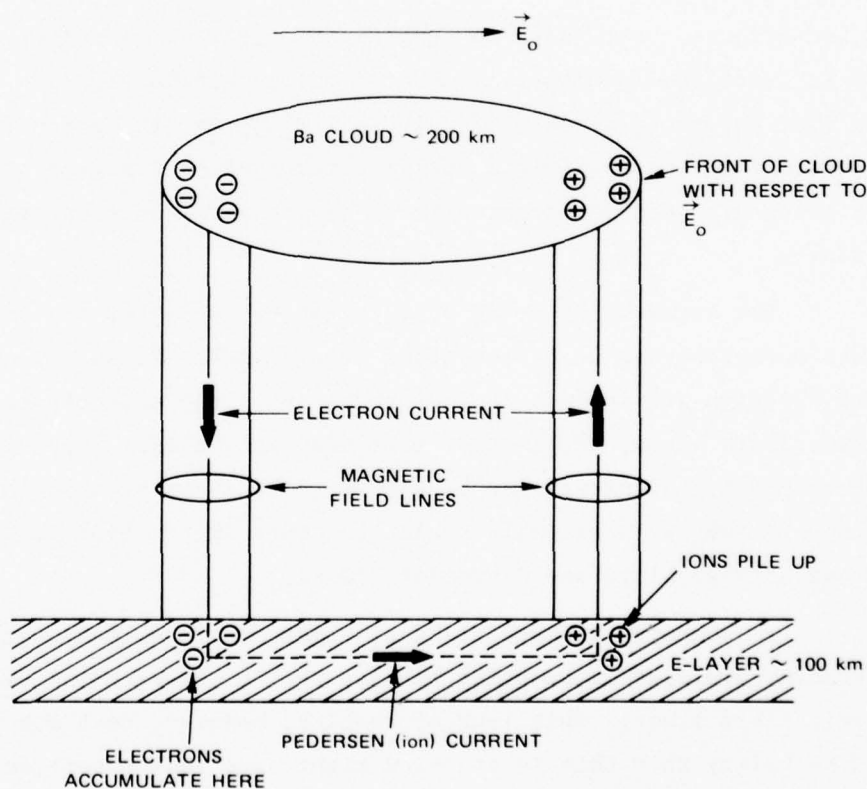


FIGURE 5 SCHEMATIC PICTURE SHOWING HOW AN F-REGION BARIUM CLOUD INTERACTS WITH THE UNDERLYING E-REGION THROUGH THE EQUIPOTENTIAL GEOMAGNETIC FIELD LINES

possibility of auroral contamination in his measurements. At any rate, Stoffregen observed that within the first minute of release photometric measurements near the foot of the magnetic field line passing through the barium cloud reveal a rapid buildup of 5577-Å emissions that reaches a maximum and then decreases to the background level. The duration of the event was generally only a few tens of seconds, with maximum intensity occurring about 10 s after the barium release. Apparently because the degree of interaction is proportional to the peak density of the ion cloud, the E-region effect rapidly decreases as the ion cloud diffuses. Hence, observation after the first minute or so does not produce measurable results (Stoffregen, 1970).

Although the SECEDE and STRESS series utilized barium releases with larger yields than those reported by Rieger et al (1968) of the Max Planck Institute, and hence would be expected to produce larger and longer E-region effects, there were no experiments (optical or radio) to observe these interactions in either the SECEDE or the STRESS programs. Thus, except for papers by Mende (1970, 1971a, 1971b) and by Landshoff (1971) which described the possible E-region effects of an F-region barium release there has been no recent effort, experimental or theoretical, on the topic.

The interest in E-region interaction is due to its part in the overall understanding of barium-cloud development. In addition, if the E- and F-region are in fact coupled together by the equipotential geomagnetic field lines, small-scale irregularities that are produced in the E-region by turbulence can be projected into the F-region cloud and can thus be the cause of small-scale structure (Reid, 1968; Volk and Haerendel, 1971; Lloyd and Haerendel, 1973).

In summary, we have found on ionograms no evidence of E-region enhancement produced by coupling between the E- and F-region via the geomagnetic field lines. This lack of results, however, does not rule out the possibility that this interaction might have gone unnoticed because experiments were not optimized to detect the effect of E-region enhancement.



## B. Reflection of Radio Waves by Barium Ionization

Perhaps two of the most puzzling features of sporadic-E returns and indeed of ionospheric returns from barium releases are the frequency extent of the traces and the maximum frequency reflected. Often the latter value is much greater than the critical frequency of the F-layer, and, if converted to a peak electron concentration with the formula  $f_c^2 = 80.1 N$ , it results in an unrealistically high value. ( $f_c$  is the critical frequency of the layer in Hz, and  $N$  is the peak density in  $\text{el}/\text{m}^3$ .)

For example, if the 15-MHz maximum frequency observed for Fb in ANNE at R + 47 min is interpreted as a critical frequency, the resulting peak density of the layer would be  $3 \times 10^{12} \text{ el}/\text{m}^3$ . If density decays as  $t^{-1/2}$ , as required by ambipolar diffusion along the geomagnetic field lines, an initial peak density of  $2 \times 10^{14} \text{ el}/\text{m}^3$  would be required. This value is about an order of magnitude greater than that generally accepted for a 48-kg barium release at 185 km altitude.

The proper interpretation of barium-associated returns seen on ionograms rests on knowledge of the physical nature of the reflecting layer and in particular on whether radio signals are reflected or scattered from the layers. As we shall see, a definitive answer to this question cannot be given because the available data appear to be consistent with at least two different models.

A key parameter in any discussion of radar target characteristics is the radar cross section (RCS) of the target. This quantity is derived from the system constants of the radar (antenna gain, frequency, etc.) and from measured parameters (range and received power). Unfortunately, while the vertichirp does provide range measurements (virtual height as a function of frequency), it was not configured to provide amplitude information. Thus, with the receiver set on AGC (automatic gain control) and with no provisions made to record the AGC voltage or to calibrate the intensity of the ionograms, it is now only possible to make a crude estimate of the strength of the barium-associated returns.

Laboratory measurements made after the completion of the STRESS experiments showed that the vertichirp sounder is able to measure a signal level of approximately -140 dBm over the range of frequencies used. To convert this signal to a minimum radar cross section we use the radar equation

$$P_R = \frac{P_T G^2 \lambda^2 K L \sigma}{(4\pi)^3 R^4}$$

where

$P_R$  = Received signal strength

$P_T$  = Transmit power (8 watts)

$G$  = Antenna gain (3 dB)

$\lambda$  = Wavelength (30 m at 10 MHz)

$K$  = Modulation factor (-13.5 dB)

$L$  = Two-way absorption and other losses (-3 dB)

$\sigma$  = Radar cross section (RCS)

$R$  = Range of the target (200 km).

Several of the numbers in the above list, the antenna gain, the D-region absorption and other losses, and the measured signal strength are not known, and estimates were made. The modulation factor,  $K$ , results from gain weighting used in the transmitter and receiver, and from the duty cycle of the transmitted signal. Thus, at a frequency of 10 MHz the RCS of the barium cloud is

$$\sigma(\text{dB m}^2) = P_R(\text{dBm}) + 187 \text{ dB}.$$

Using the laboratory measurement of -140 dBm for  $P_R$  we conclude that under ideal conditions the vertichirp should be able to detect the cloud if it has an RCS of at least 47 dB relative to  $1 \text{ m}^2$ , or  $5 \times 10^4 \text{ m}^2$ .

Measurements of barium-cloud radar cross section in the 5-to-10-MHz range during SECEDE II and III indicate that the cross section of a typical 48-kg cloud reaches a peak of about  $10^6 \text{ m}^2$  shortly after release

and decays to about  $10^5 \text{ m}^2$  in about 10 to 15 min. The RCS is not well behaved, and 5-to-10-dB excursions in a one-minute period can occur. Nevertheless, during the first 10 min following release,  $2 \text{ to } 3 \times 10^5 \text{ m}^2$  appears to be a representative RCS. Late-time data when the ion cloud is fully striated apparently do not exist, but in view of the strength of the late-time echoes seen in Event ANNE, the RCS must remain above  $10^5 \text{ m}^2$  for tens of minutes.

Cross sections for the layers causing the E-region returns are not available, but based on their appearance on the ionograms we estimate that the received signal power is comparable for echoes from both E- and F-regions. Because of the range dependence in the radar equation, however, the RCS of the layer at 100 km can be a factor of 16 less than the RCS of a layer at 200 km and still have the same received power. Thus, the minimum detectable cross section at 100 km is about  $3 \times 10^3 \text{ m}^2$ .

Before we address the question of the reflection mechanism to be associated with the F-region returns we first note some of their characteristics:

- (1) The first evidence of barium echoes occurs some time after release. During SECEDE II barium echoes were observed about 2 to 10 min after release. During STRESS, echoes occurred in the 10-to-20-min time frame.
- (2) The first echoes observed were either direct or mixed-mode echoes.
- (3) Retardation or magnetoionic splitting was generally not evident on barium returns. The traces were typically very thin and show little or no range dependence with frequency.
- (4) When the echoes were first observed they tended to be weak, but they typically increased in intensity with the passage of time.

From these observations we conclude that the returns were not due to overdense or total reflection. The reasons are as follows: HF radar measurements show that maximum cross section occurs a few minutes after release. Hence, if overdense reflection was responsible for the Fb traces the strongest returns would occur one or two minutes after release, with intensity decreasing with time. The opposite trend is observed.



Gradient reflection and scattering, either from dense blobs or weak irregularities, are two mechanisms often proposed to explain sporadic-E echoes. In applying these models to barium echoes we find that signal intensity does not permit a clear choice, since both mechanisms can lead to returned signals with comparable radar cross sections.

In terms of signal characteristics we expect gradient reflection to result in thin, discrete echoes, whereas scattering should lead to diffused returns that may at times have appreciable range depth. Since examples of both types of echoes can be found in the data, a clear choice between the two models cannot be made.

Thus we conclude that gradient reflection and scatter are viable mechanisms for the origin of Fb echoes. Because of the large minimum detectable RCS ( $5 \times 10^4 \text{ m}^2$ ) of the vertichirp, the release and initial development of the barium cloud is not visible to the ionosonde. Only when the cloud has expanded and perhaps formed sheets of sufficient cross section at the correct orientation to the ionosonde is the cloud detected. The ion cloud is highly aspect-sensitive and at times a mixed-mode echo is observed because its path presents a larger cross section than the direct path.

The characteristics of the E-region echoes observed during FERN are quite similar to those summarized for the Fb returns with the following additions:

- (1) Blanketing of the upper layers was not observed for any of the STRESS releases. Blanketing occurred on three of the six releases in SECEDE II.
- (2) FERN showed a clear descent of the echoing layer from the F-region to the lower E-region. This trace started as a weak return but later became very intense.

Blanketing was not observed during FERN, possibly because the layer density was too low, or because the layer did not pass directly overhead. The layer's peak density is not well known, but the SECEDE II results suggest that  $3 \times 10^{11} \text{ m}^{-2}$  (5 MHz critical frequency) is possible even 100 min after release. Since the lack of partial blanketing for any event implies a rather limited horizontal extent for the Eb layer we conclude

that the peak density region of the FERN Eb layer probably did not pass over the ionosonde.

The strength of the FERN Eb returns and their time characteristics suggest that the returns are due to thin layers with high gradients. The underside of these layers, however, cannot be smooth; if they were, returns would not be possible unless these layers were directly overhead. The best model for the Eb layers seems to be a thin, rough layer with high gradients.

#### IV CONCLUSIONS

Analysis of ionograms obtained during the Pre-STRESS and STRESS program in concert with other pertinent data and sporadic-E theories yield the following observations and conclusions:

- (1) Characteristics of barium-associated ionosonde traces
  - (a) F-region echoes (Fb echoes)
    - Evidence of barium cloud first occurs some time after release. During SECEDE II, barium echoes were observed about 2 to 10 min after release. During STRESS, echoes occurred in the 10-to-20-min time frame.
    - The first echoes observed were either direct or mixed-mode echoes.
  - (b) E-region echoes (Eb echoes)
    - FERN showed a clear descent of the echoing layer from the F-region to the lower E-region. This E-region trace subsequently became very intense, reached a minimum range of 105 km, receded, and then faded out.
    - Blanketing of the upper layers was not observed during any of the STRESS releases. Blanketing occurred on three of the six SECEDE II releases.
  - (c) E- and F-region echoes
    - Retardation and magnetoionic splitting were generally not observed. The traces were typically very thin and showed little or no range dependence with frequency.
    - When the echoes are first observed they tend to be weak, but they typically increase in intensity with time.
- (2) Nature of the layers responsible for the barium-associated returns
  - (a) The direct and mixed-mode returns in the F-region originated from the barium ion cloud.
  - (b) Mixed-mode echoes are due to the aspect-sensitive nature of the ion cloud.
  - (c) In the E-region the returns are from layers of barium ions that separate from the main cloud and descend to the E-region through the combined action of gravity, a northern component of the neutral wind, and/or a westward component of the electric field.

- (d) Once the barium ions descend to the E-region they are compressed into thin layers, with a corresponding increase in cross section.
- (3) Reflection or scattering mechanism responsible for the echoes
  - (a) The nature of the reflection layer can be best described as a thin layer of barium ions with sharp upper and lower boundaries.
  - (b) Gradient reflection is the most likely mechanism, but other possibilities such as scattering from weak irregularities or from dense blobs cannot be ruled out.
  - (c) Reflection is not specular, so maximum frequency observed for the layer cannot be interpreted as a critical or a maximum plasma frequency.
- (4) Coupling of E- and F-Region. E-region interactions with the F-region cloud through electrodynamic coupling via the equipotential field lines are not supported by the data.

## REFERENCES

- Axford, W. I., "The Formation and Vertical Movement of Dense Ionized Layers in the Ionosphere due to Neutral Wind Shears," J. Geophys. Res., Vol. 68, pp. 769-779 (1963).
- Baender, R., "Vertical-Incidence-Sounder Observations During SECEDE II," Stanford Research Institute (Unpublished).
- Booker, H. G. and W. E. Gordon, "A Theory of Radio Scattering in the Troposphere," Proc. IRE, Vol. 38, pp. 401-412 (1950).
- Chang, N. J. F., "SECEDE III Ionograms Revisited," Stanford Research Institute (Unpublished).
- Dungey, J. W., "The Influence of the Geomagnetic Field on Turbulence in the Ionosphere," J. Atmos. Terr. Phys., Vol. 8, pp. 39-42 (1956).
- Dungey, J. W., "Effect of a Magnetic Field on Turbulence in an Ionized Gas," J. Geophys. Res., Vol. 64, pp. 2188-2191 (1959).
- Gordon, W. E., "Incoherent Scattering of Radio Waves by Free Electrons with Applications to Space Exploration by Radar," Proc. IRE, Vol. 46, pp. 1824-1829 (1958).
- Haerendel, G., R. Lust, and E. Rieger, "Motion of Artificial Ion Cloud in the Upper Atmosphere," Planet. Space Sci., Vol. 15, pp. 1-18 (1967).
- Landshoff, R. K., "Interactions Between the Barium Cloud and the E Layer," Stanford Research Institute (Unpublished).
- Lloyd, K. H. and G. Haerendel, "Numerical Modeling of the Drift and Deformation of Ionospheric Plasma Clouds and of Their Interaction with Other Layers of the Ionosphere," J. Geophys. Res., Vol. 78, pp. 7389-7415 (1973).
- MacLeod, M. A., "Sporadic E Theory. I. Collision-Geomagnetic Equilibrium," J. Atmos. Sci., Vol. 23, pp. 96-109 (January 1966).



Mende, S. B., "Estimate of Induced E-Region-Irregularity Enhancement," Stanford Research Institute (Unpublished).

Mende, S. B., "Generation of Secondary Irregularities by Motion of Ion Clouds," Stanford Research Institute (Unpublished).

Mende, S. B., "Observation of Current System and Striation Formation Mechanism," Stanford Research Institute (Unpublished).

\* Miller, K. L. and L. G. Smith, "Midlatitude Sporadic-E Layers," Aeronomy Report No. 76, IULU-ENF 76 2507/, University of Illinois, Urbana, Illinois (December 1, 1976).

Oetzel, G. N. and N. J. F. Chang, "Analysis of SECEDE III HF Data," RADC-TR-69-412, Contract F30602-68-C-0076, Stanford Research Institute, Menlo Park, Calif. (November 1969).

Radio Science, Vol. 10, No. 3, Special Issue: "Recent Advances in the Physics and Chemistry of the E Region" (March 1975).

Radio Science, Vol. 7, No. 3, Special Issue: "Papers Presented at Third Seminar on the Cause and Structure of Temperate Latitude Sporadic E" (March 1972).

Radio Science, Vol. 1, Special Issue on Sporadic-E (February 1966).

Reddy, C. A. and M. M. Rao, "On the Physical Significance of the Es Parameters fbEs, and foEs," J. Geophys. Res., Vol. 73, pp. 215-224 (1968).

Reddy, C. A., "Physical Significance of the Es Parameters fbEs, fEs, and foEs, 2. Causes of Partial Reflections from Es," J. Geophys. Res., Vol. 73, pp. 5627-5647 (1968).

Reid, G. C., "The Formation of Small-Scale Irregularities in the Ionosphere," J. Geophys. Res., Vol. 73, pp. 1627-1640 (1968).

---

\* References containing extensive bibliographies are marked with an asterisk (\*). This distinction has also been used to indicate works of a comprehensive or survey nature.

- Rieger, E., H. Foppl, G. Haerendel, L. Haser, J. Loidl, R. Lust, F. Melzner, B. Meyer, and H. Neuss, Final Report on Experiment R-33 in ESRO-Payload S 04, Max Planck Institute Fur Aeronomie, West Germany (January 1968).
- Simons, J. J., "Event OLIVE--Ionosonde Late-Time Observations," Stanford Research Institute (Unpublished).
- Simons, J. J., "Preliminary Ionosonde Observations during SECEDE II," Stanford Research Institute (Unpublished).
- \* Smith, E. K., Jr. and S. Matsushita, Eds., Ionospheric Sporadic E (The MacMillan Co., New York, N.Y., 1962).
- Stoffregen, W., "Electron Density Variation Observed in the E-layer Below an Artificial Barium Cloud," J. Atmos. Terr. Phys., Vol. 32, pp. 171-177 (1970).
- Thome, G. D., "The OLIVE Working Group--A Summary of Findings," Stanford Research Institute (Unpublished).
- Volk, H. J. and G. Haerendel, "Striations in Ionospheric Ion Clouds, 1," J. Geophys. Res., Vol. 76, pp. 4541-4559 (1971).
- \* Whitehead, J. C., "Production and Prediction of Sporadic E," Rev. Geophys. Space Phys., Vol. 8, pp. 65-144 (1970).
- Whitehead, J. D., "The Formation of the Sporadic-E Layer in the Temperate Zone," J. Atmos. Terr. Phys., Vol. 20, pp. 49-58 (1961).

---

\* See footnote on previous page.

Appendix A  
IONOSPHERIC DATA

## Appendix A

### IONOSPHERIC DATA

The Barry Research VIS-1 Vertichirp sounder that was fielded in support of the STRESS experiments is a frequency-modulated FM (chirp) radar designed to perform vertical-incidence ionospheric soundings. The sounder has a frequency range from 0.5 to 30 MHz and a virtual-height range of 0 to 1000 km. A single-wire delta antenna was used for transmitting and receiving.\* Transmitted power was 3 watts average, and 8 watts peak. Various sweep formats and other operational parameters can be chosen to suit any likely ionospheric conditions, but in general, the sounder was operated using the following parameters:

- Linear sweep rate--50 kHz/s
- Lower frequency limit--0.5 Mhz
- Upper frequency limit 10, 15, or 20 MHz, depending on the extent of the barium returns
- Hourly operation except on release days when the sounder was in continuous operation.

The vertical ionosonde was located at Eglin Site C-6 adjacent to the Technology International Corporation photographic site and the TV-track site. The equipment shared the TV-track van.

During Pre-STRESS the vertichirp started operation on 29 November at 2134 UT and provided coverage of the ANNE release on 1 December 1976. The equipment was shut down after the completion of this single Pre-STRESS test, and resumed operation on 20 February 1977 at 2116 UT for

---

\* Since a broadband delta was not used, system sensitivity was probably degraded at low frequencies. Construction of a broadband delta antenna by range support was requested in the contract but was not accomplished. Thus, with the limited personnel and equipment that was available on site a simpler antenna was erected.

the STRESS experiments. From this time the ionosonde operated on an hourly schedule until the completion of the last STRESS release on 14 March 1977. On release days, as summarized in Table A-1, the normal hourly schedule was changed to a continuous mode, which typically produced a new ionogram every 3 minutes.

Table A-1  
SUMMARY OF PRE-STRESS AND STRESS RELEASES

Event	Release Time (UT)	Date (UT)
ANNE	2311:42	1 December 1976
BETTY	2352:27	26 February 1977
CAROLYN	2352:10.5	2 March 1977
DIANNE	0001:08	8 March 1977
ESTHER	2301:08.8	13 March 1977
FERN	2246:08.8	14 March 1977

A concise summary of the ionospheric conditions on the six barium release days is given by the f-plots presented in Figures A-1 through A-6. The critical frequencies shown for the E- and F-layers were scaled from the ionograms. The uncertainty in reading the critical frequencies is about  $\pm 0.1$  MHz when the layers are well defined. Generally, accuracies are within about  $\pm 0.2$  MHz.

Ionograms for the barium releases that produced ionospheric echoes are shown in Figures A-7 through A-11. In Figure A-7, Fb echoes are particularly strong and had a maximum frequency of 15 MHz at 2359 UT (R + 47.3 min). Several spurious returns can be seen. These occurred below about 140 km and are identified as spurious because they show no range variation with time and because they occurred during laboratory tests using known signals. Four such spurious returns can be seen at 2353 UT in Figure A-7. One started at 10 MHz at 100 km, with a symmetrical pair about this range starting at 15 MHz. The strong trace at 130 km extending from 2 to 9 MHz is also believed to be equipment-related. Thus, all of the E-region traces in ANNE are believed to be equipment-related.



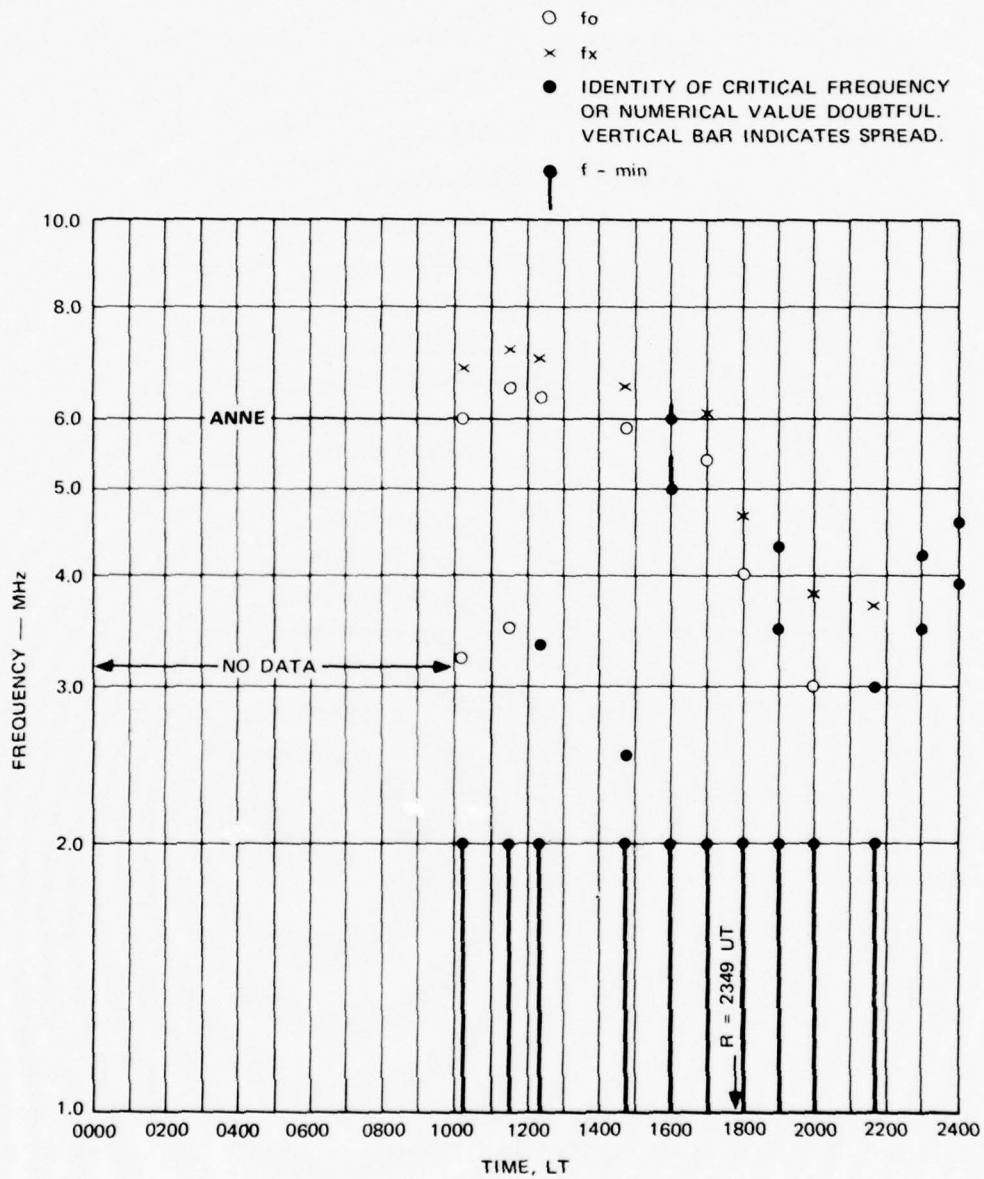


FIGURE A-1 f-PLOT FOR EVENT ANNE

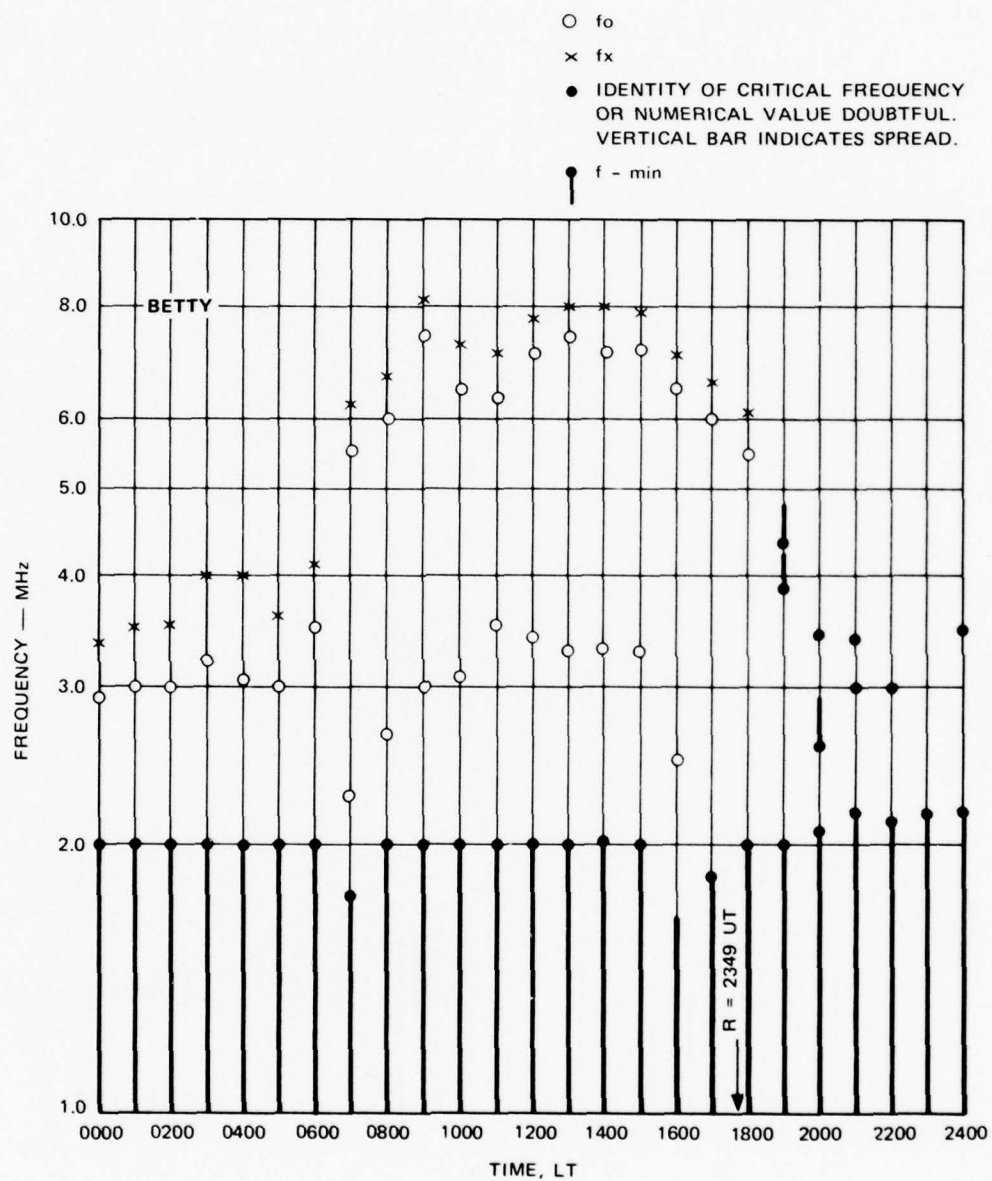


FIGURE A-2  $f$ -PLOT FOR EVENT BETTY

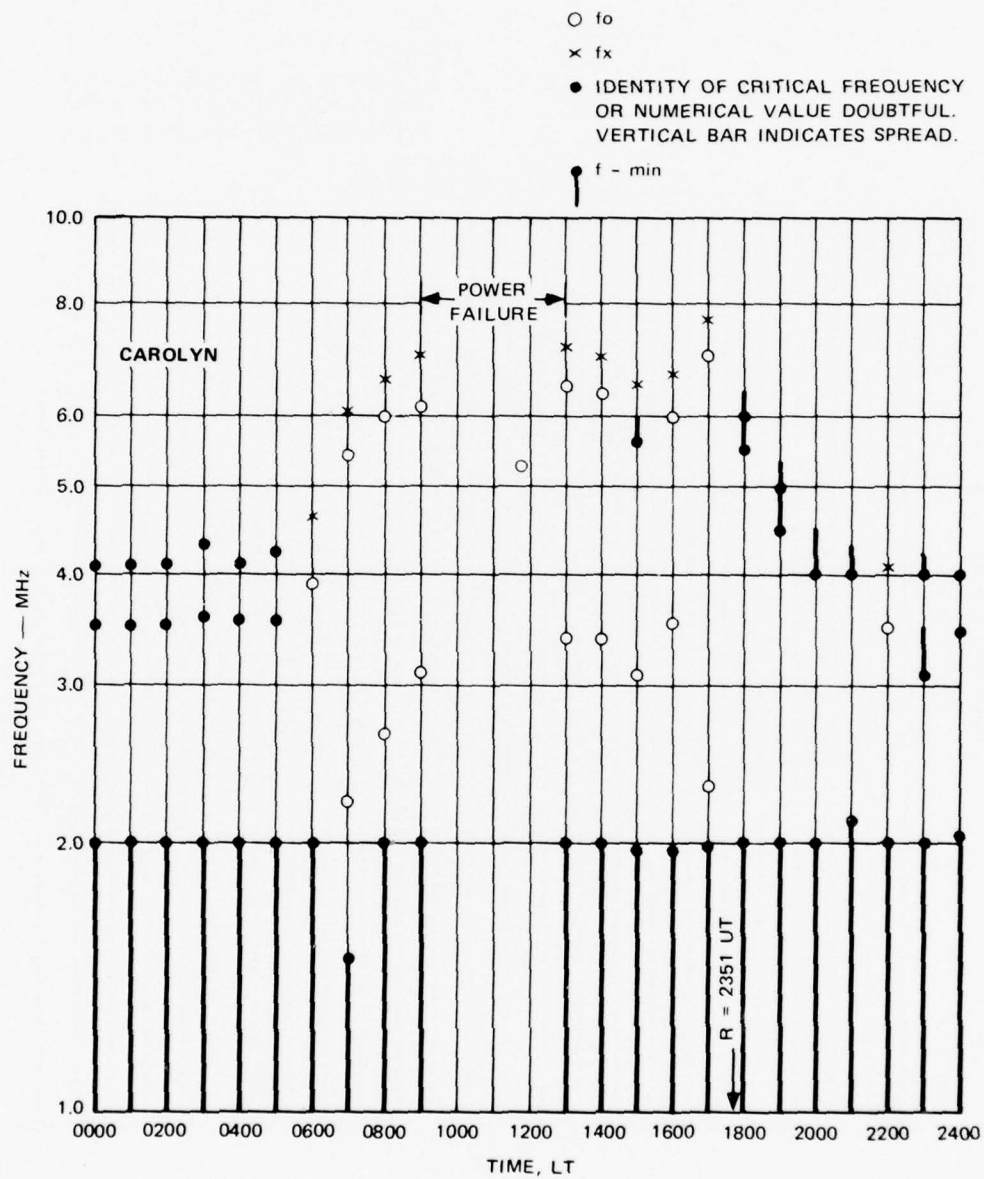


FIGURE A-3 f-PLOT FOR EVENT CAROLYN

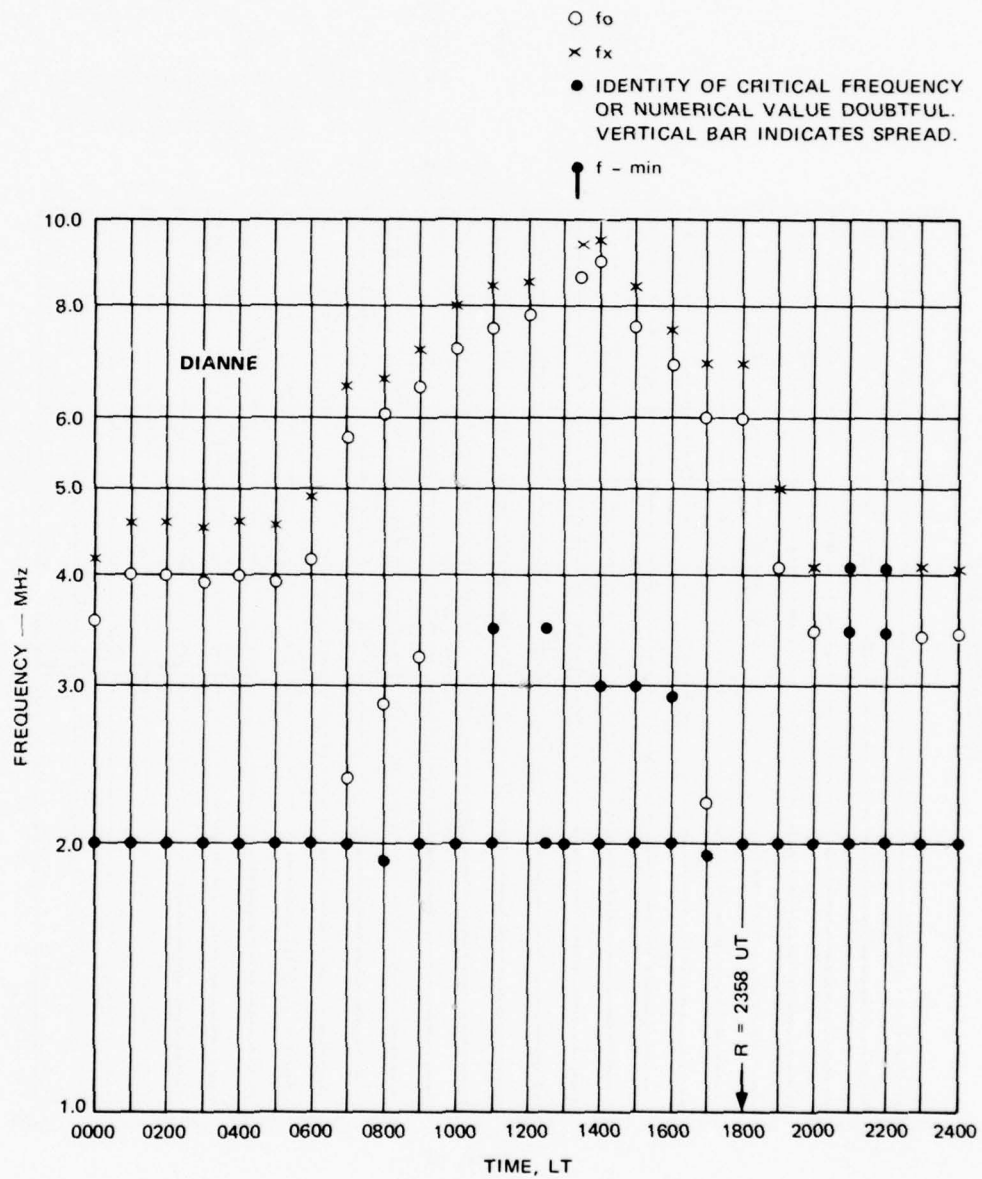


FIGURE A-4 f-PLOT FOR EVENT DIANNE

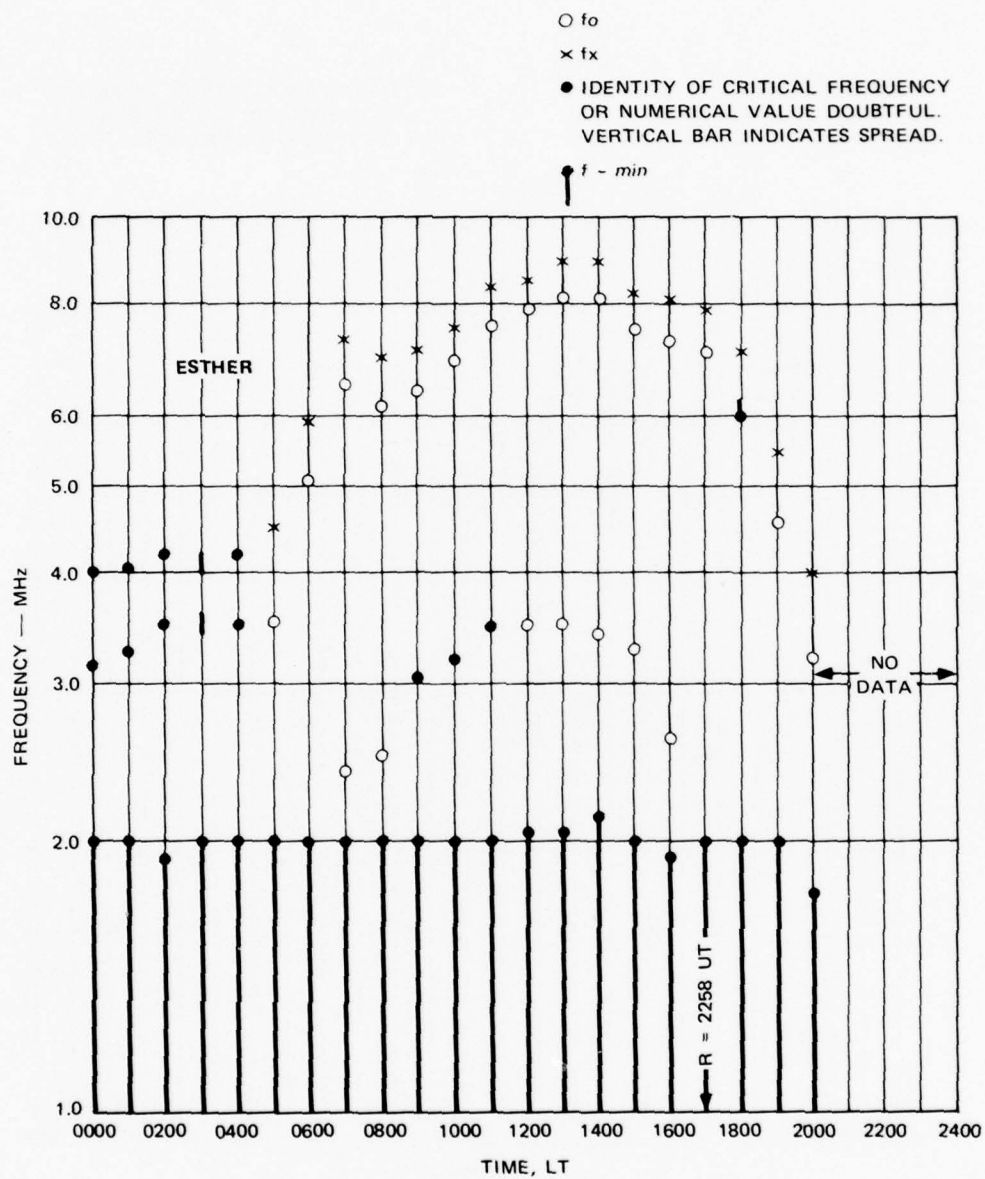


FIGURE A-5  $f$ -PLOT FOR EVENT ESTHER



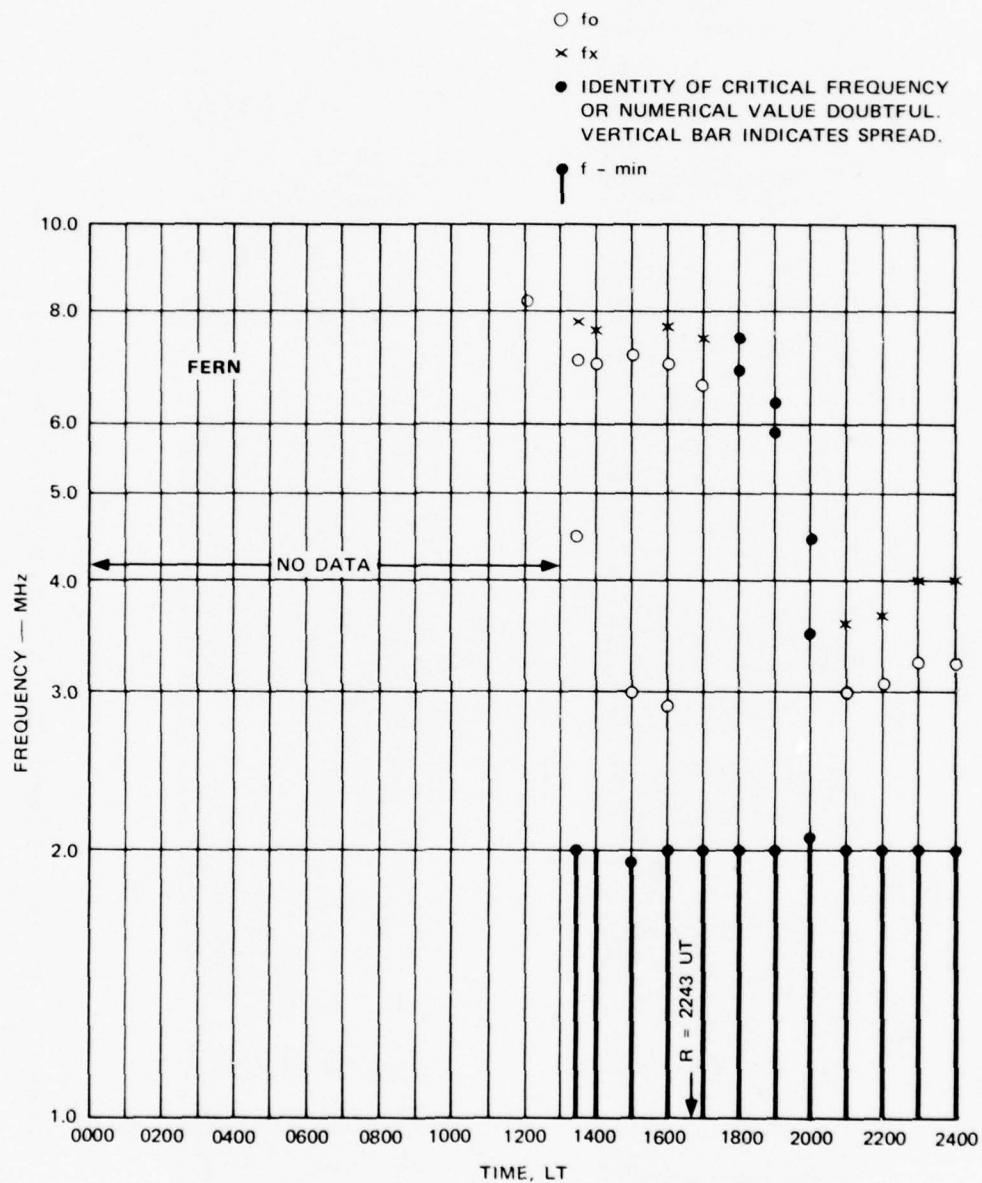


FIGURE A-6 f-PLOT FOR EVENT FERN

# ANNE

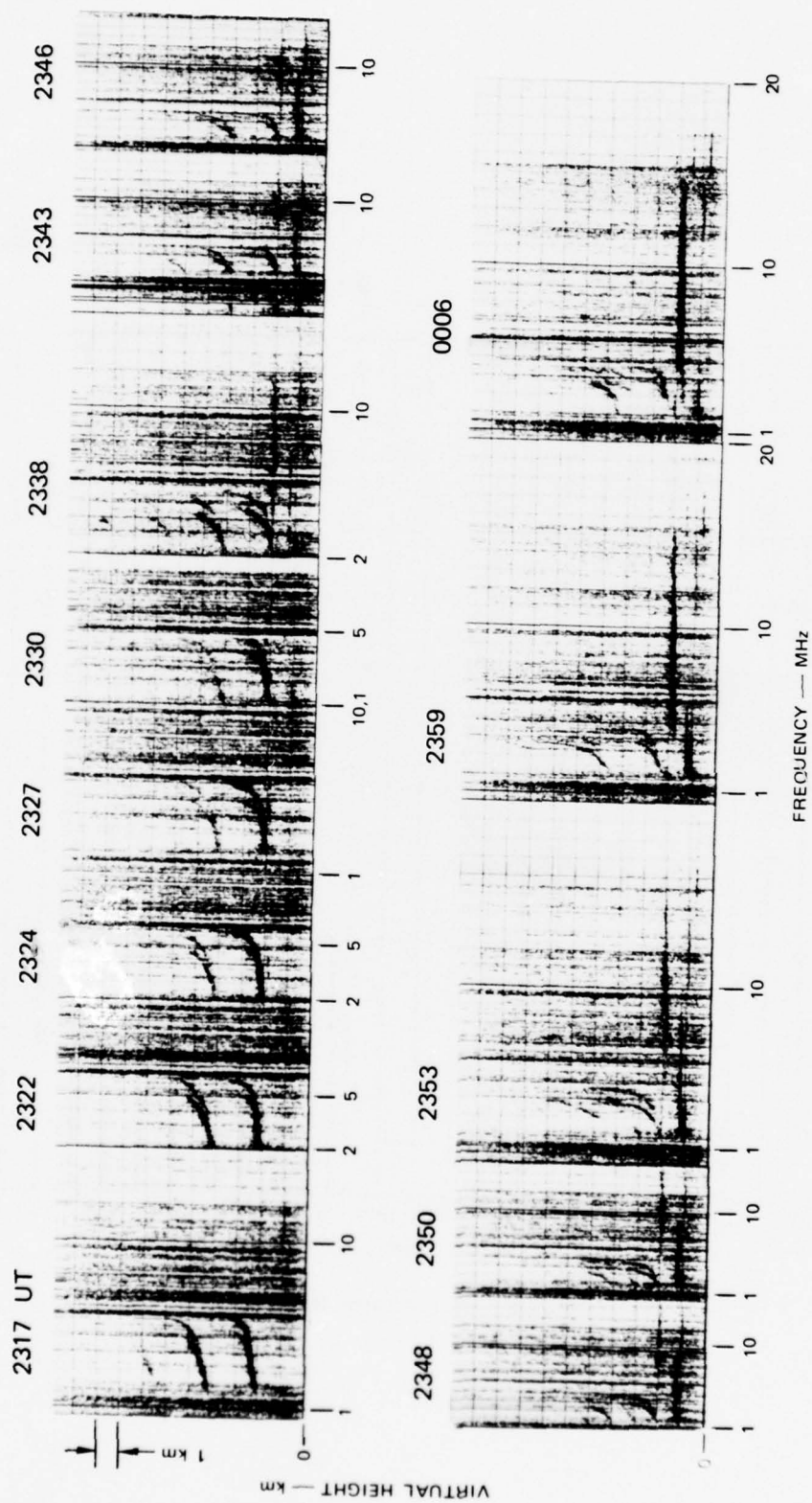


FIGURE A-7 IONOGRAMS TAKEN ON 1 AND 2 DECEMBER 1976 FOR EVENT ANNE

# ANNE

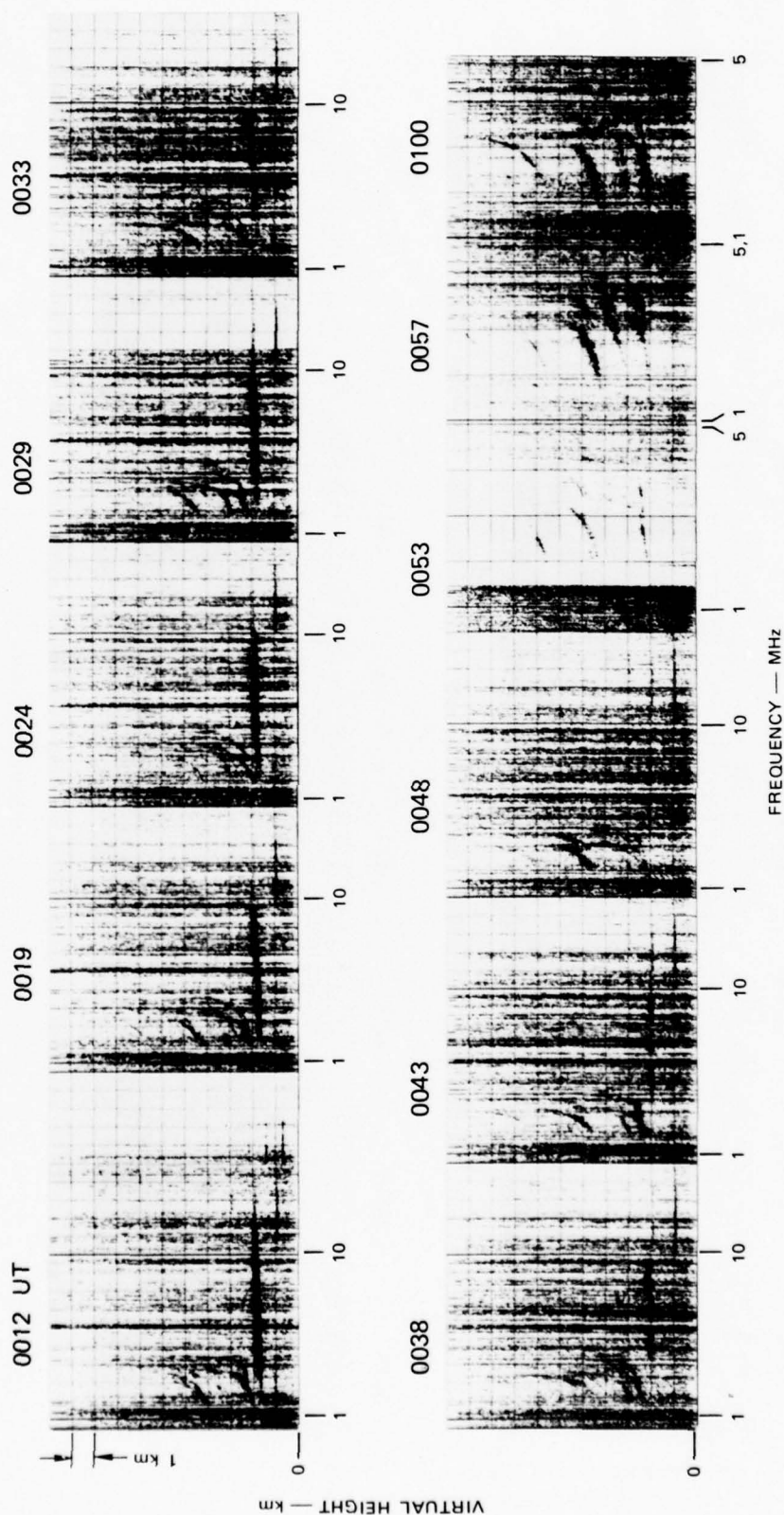


FIGURE A-7 (Concluded)

# CAROLYN

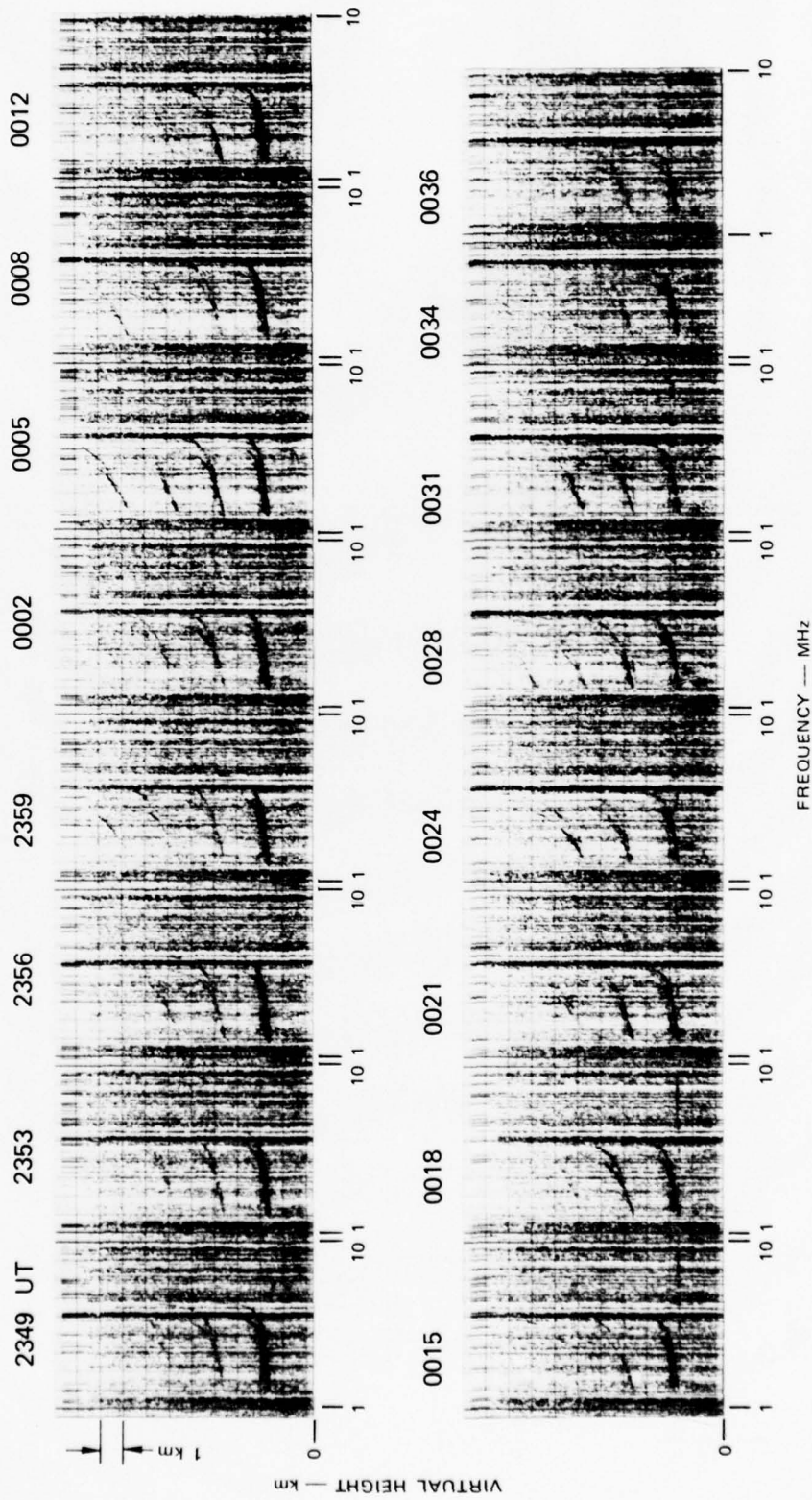


FIGURE A-8 IONOGRAMS TAKEN ON 2 AND 3 MARCH 1977 FOR EVENT CAROLYN



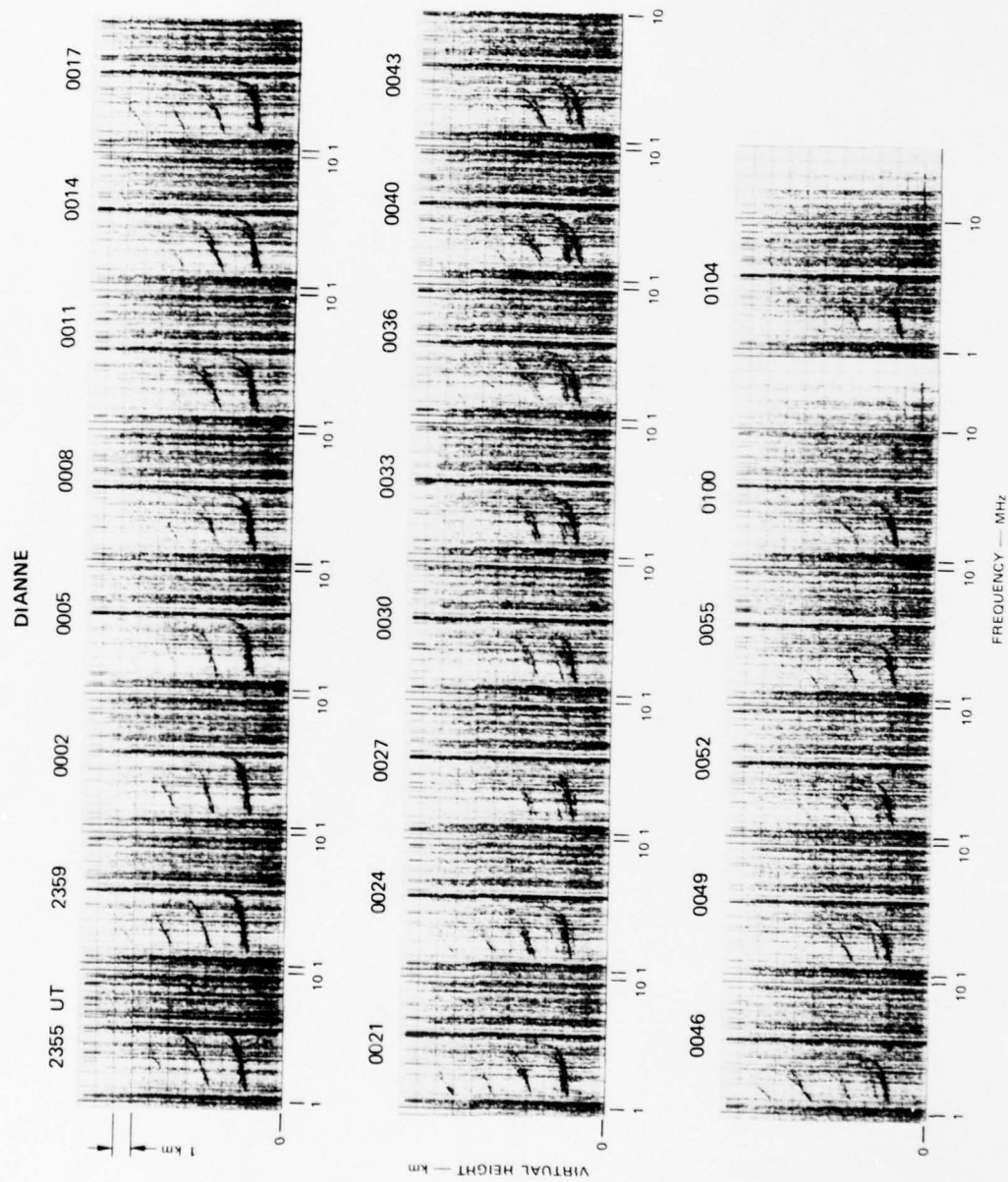


FIGURE A-9 IONOGRAMS TAKEN ON 8 AND 9 MARCH 1977 FOR EVENT DIANNE



# ESTHER

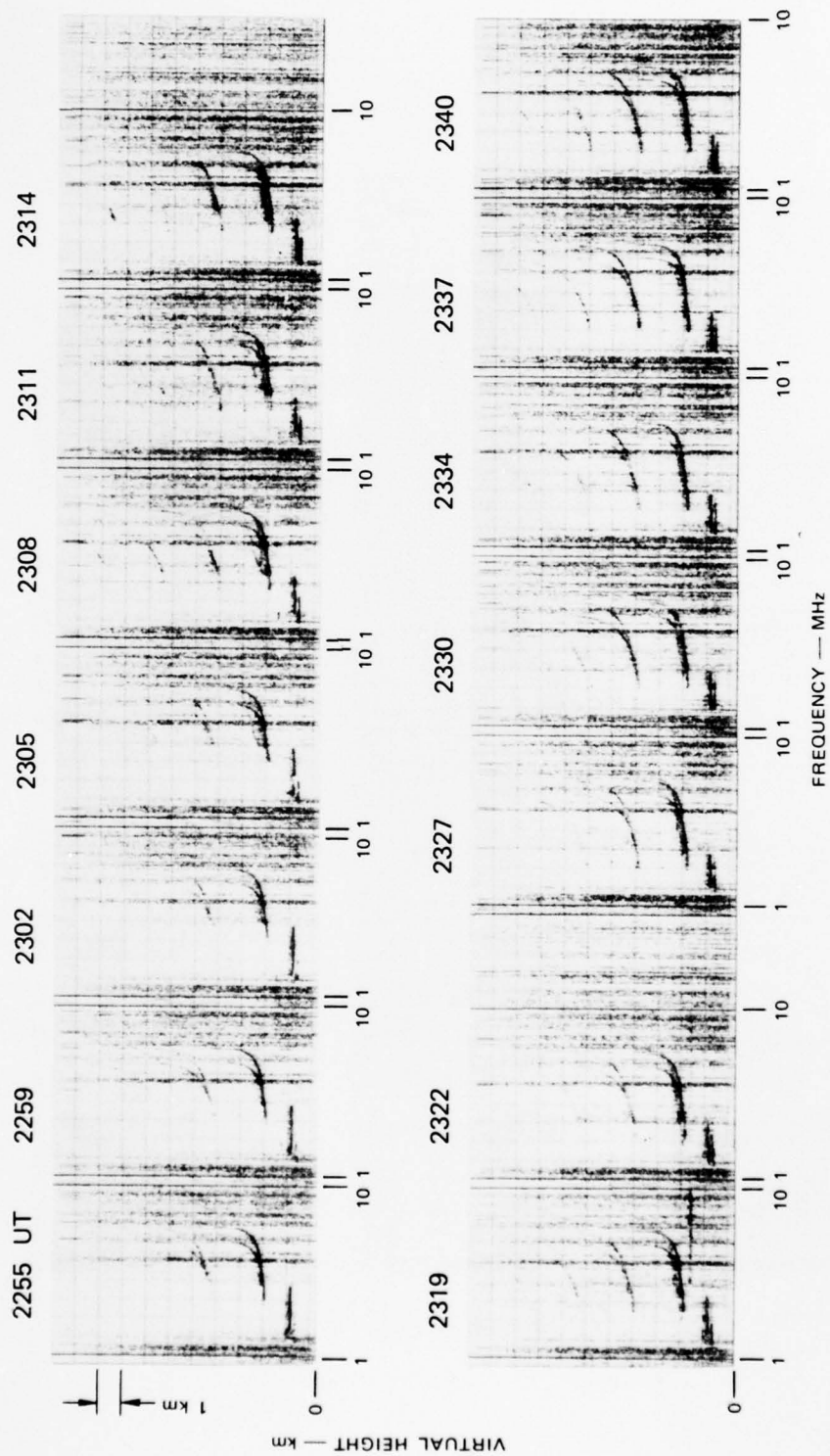


FIGURE A-10 IONOGRAMS TAKEN ON 13 AND 14 MARCH 1977 FOR EVENT ESTHER



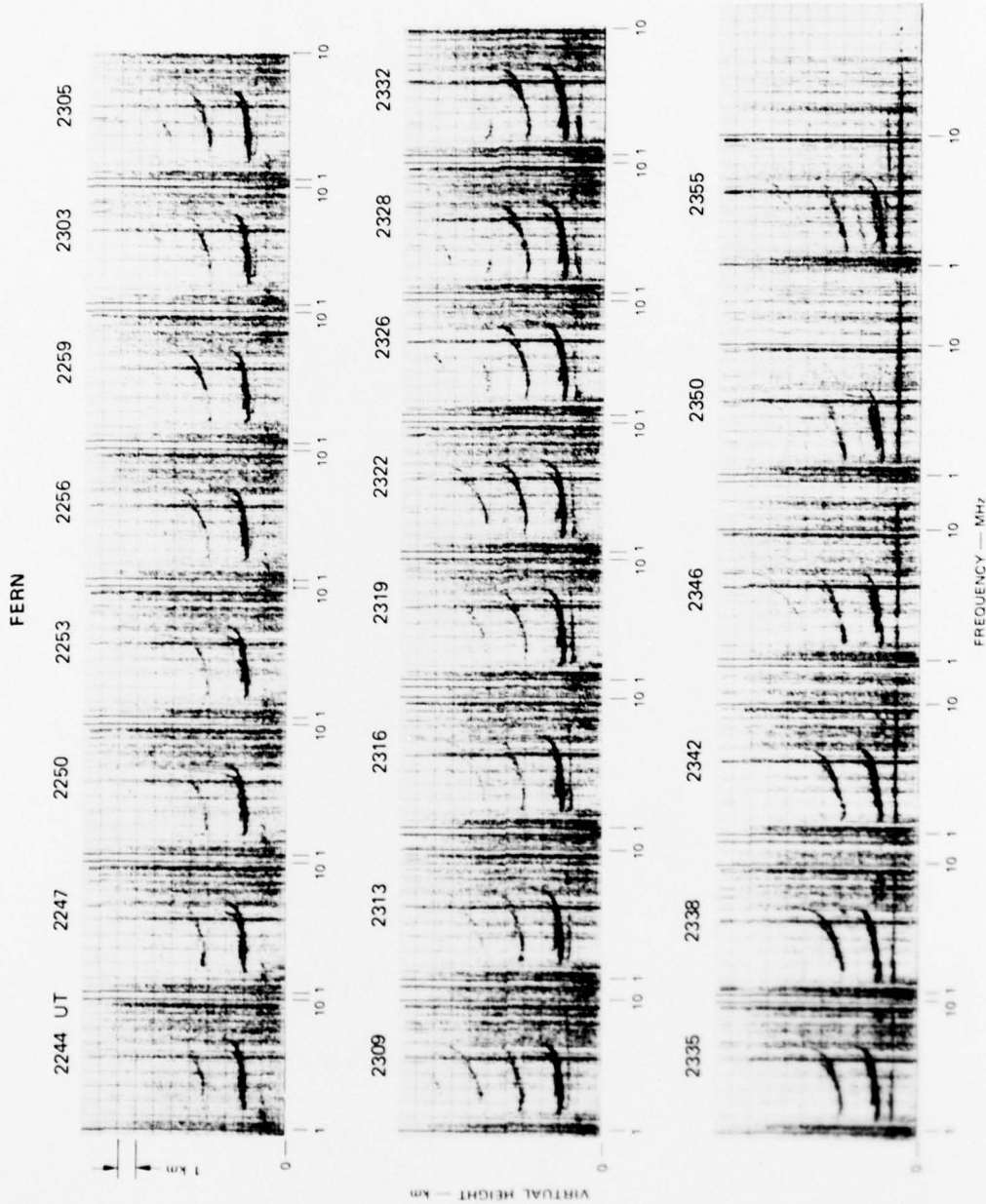


FIGURE A-11 IONOGRAMS TAKEN ON 14 AND 15 MARCH 1977 FOR EVENT FERN

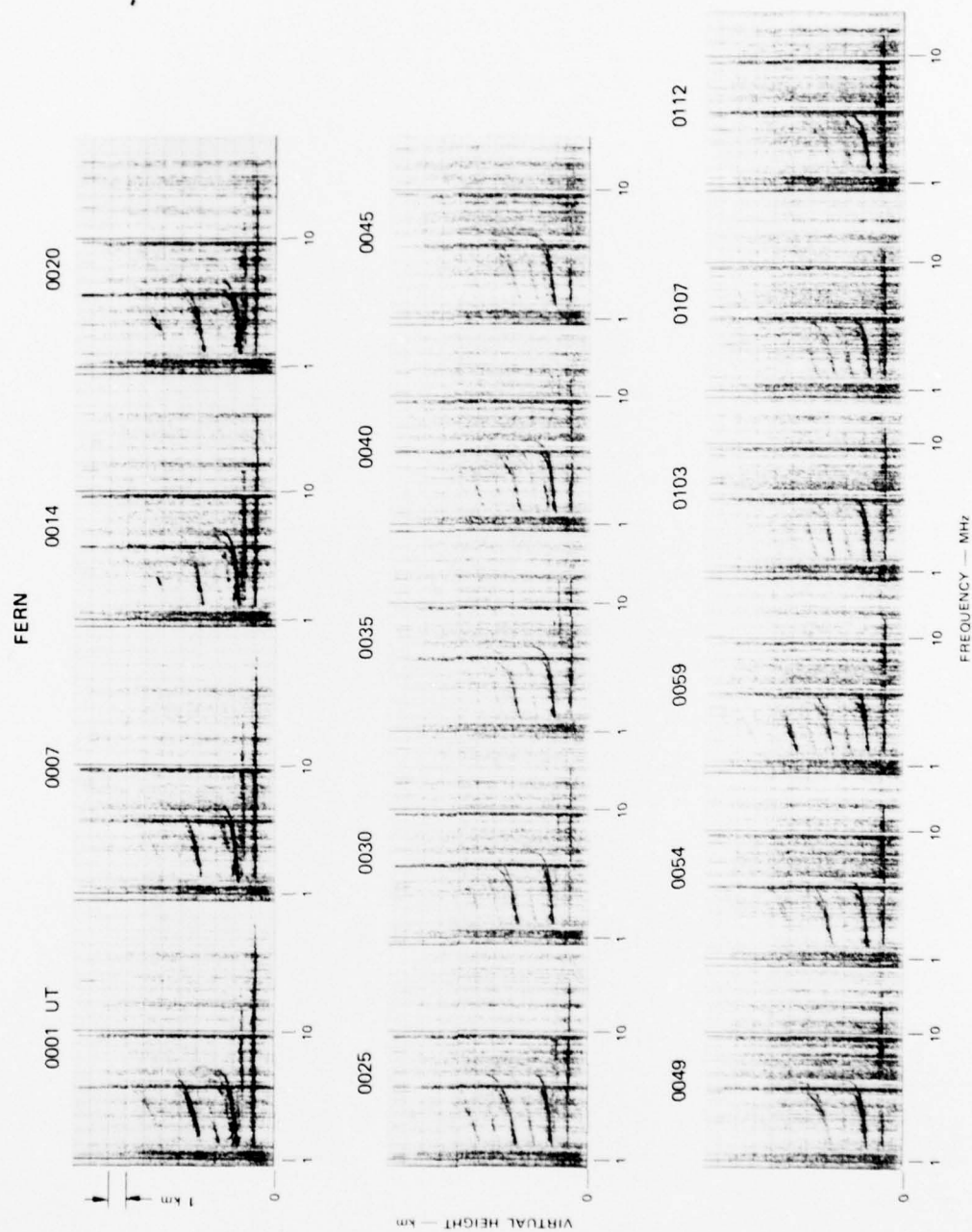


FIGURE A-11 (Continued)



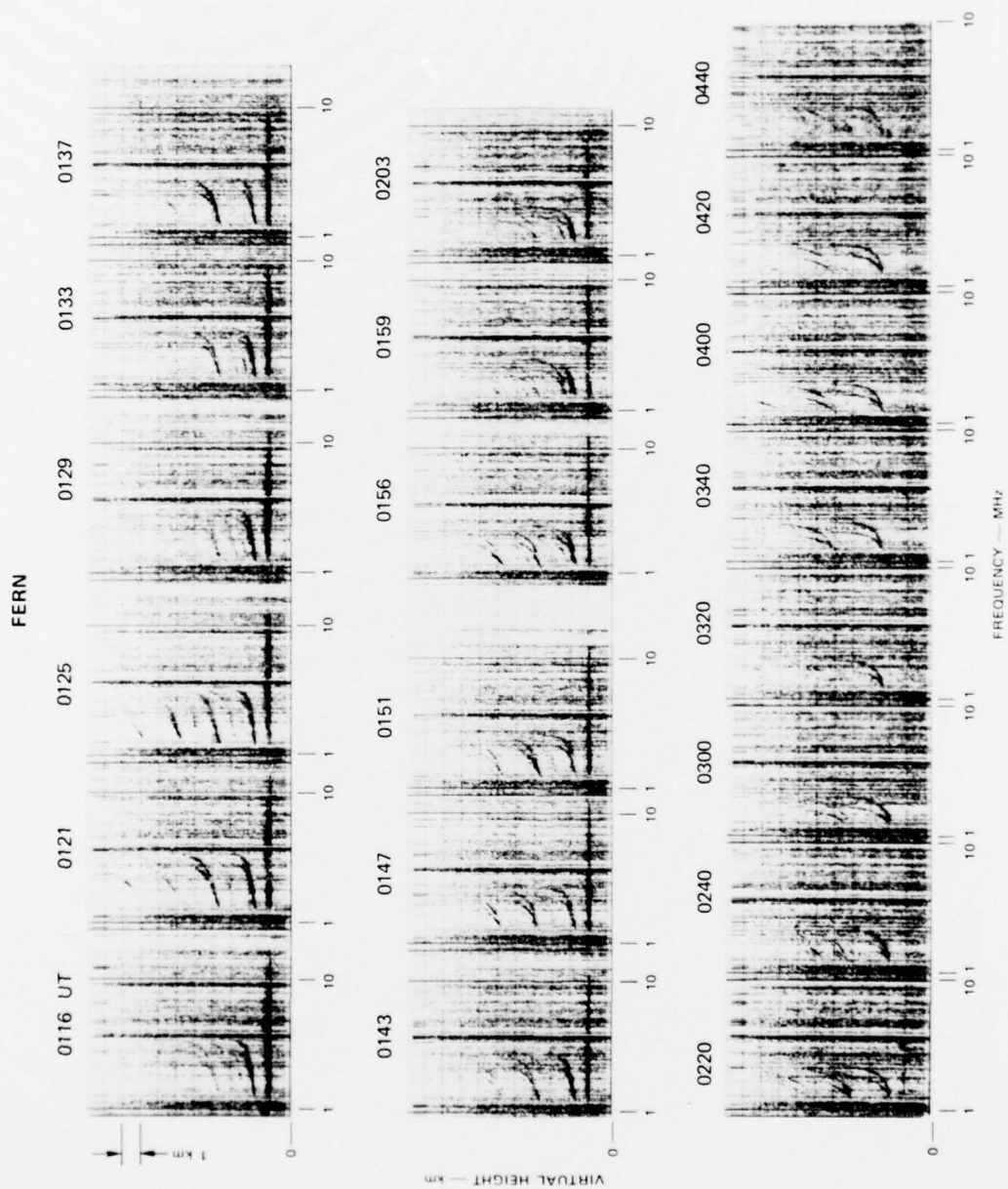


FIGURE A-11 (Continued)



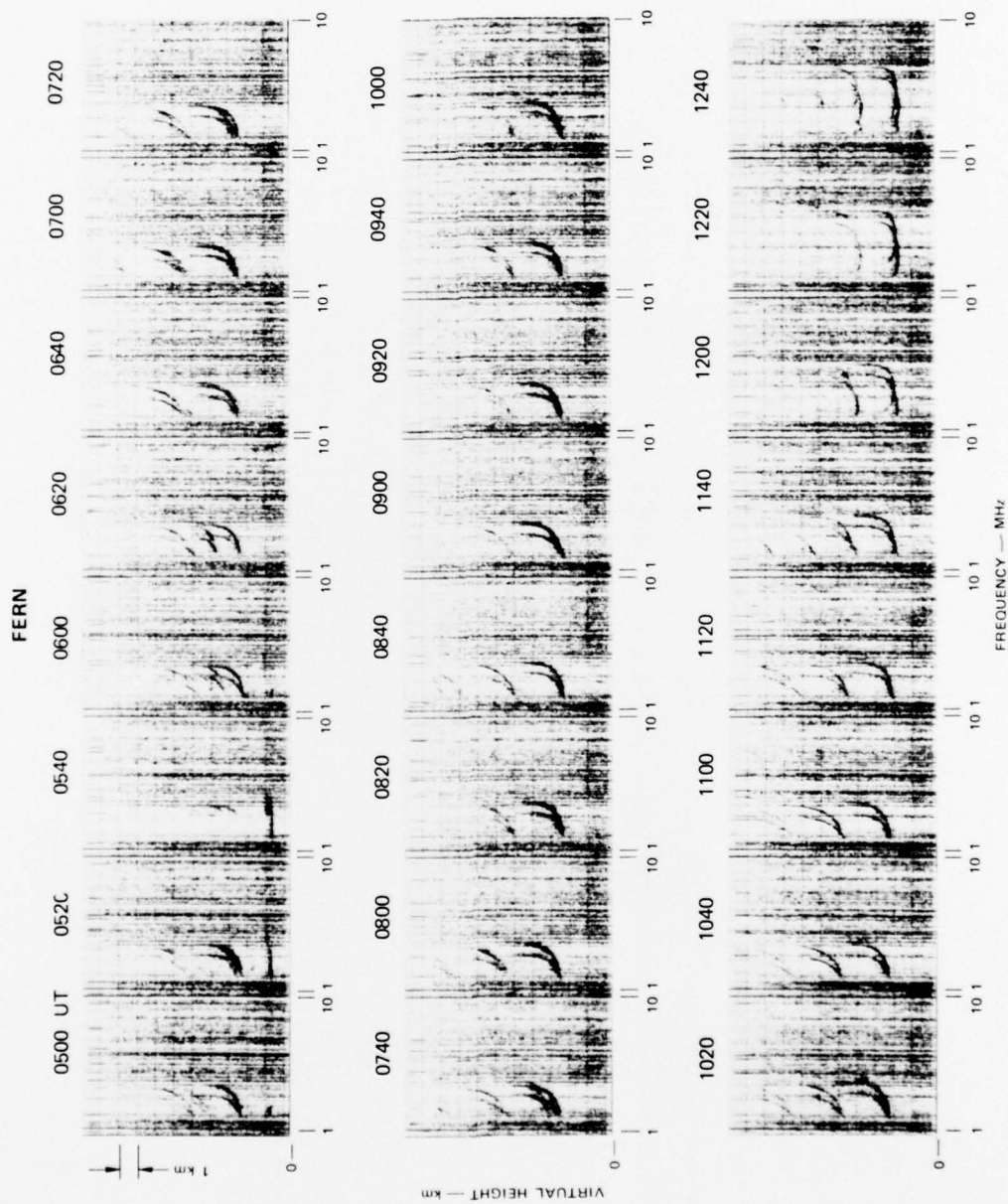


FIGURE A-11 (Continued)

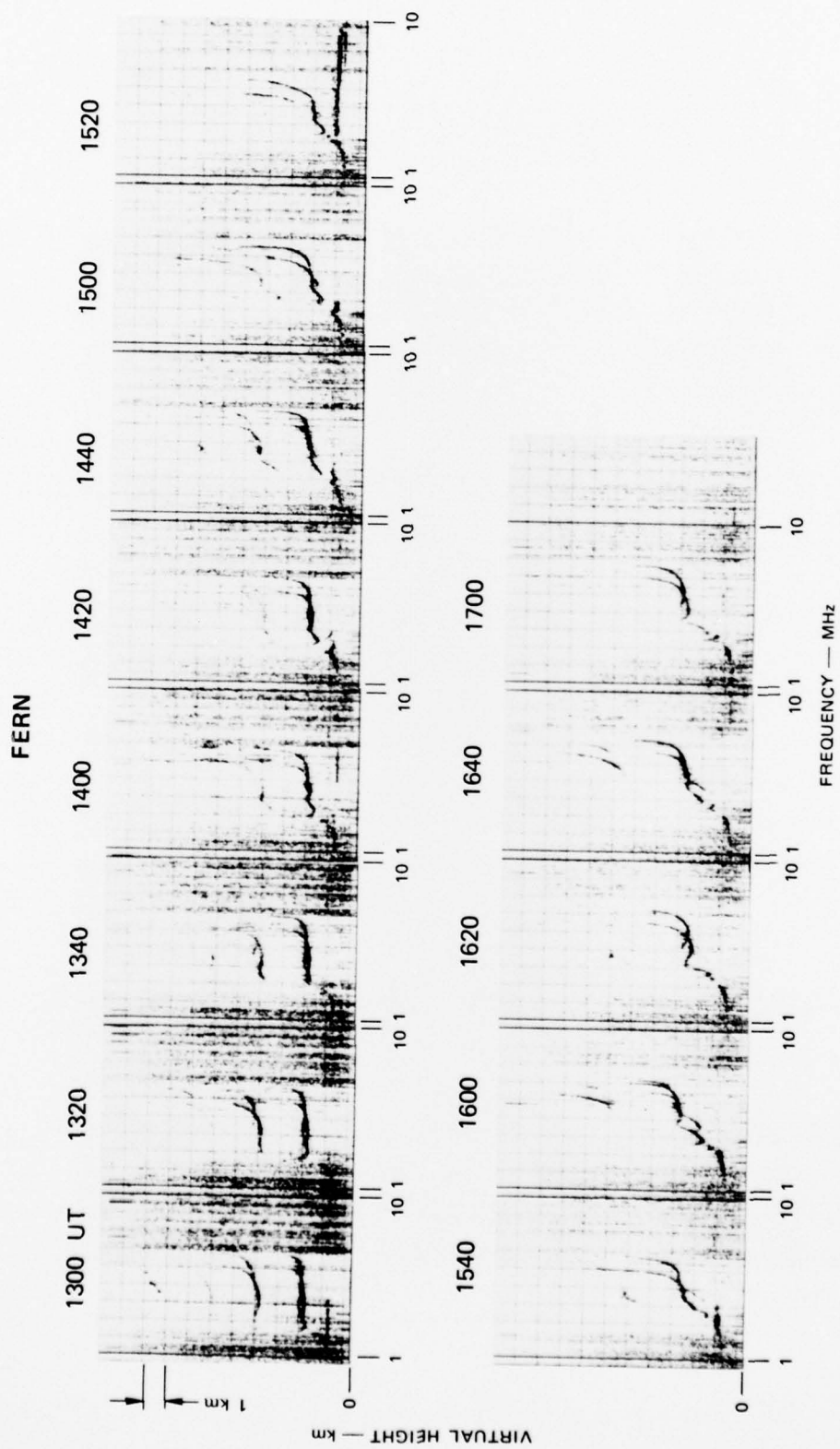


FIGURE A-11 (Concluded)

The ANNE Fb trace at 2338 UT apparently shows a slight amount of retardation at the high-frequency end of the trace. In addition, magneto-ionic splitting is apparently present near 6 and 7 MHz. This frequency ( $f_oF_b = 6.8$  MHz) can be converted into a peak density of  $6 \times 10^{11}$  e1/m<sup>3</sup>, which is about an order of magnitude less than the peak density measured by the FPS-85 at R + 47.3 min. If we convert the maximum frequency observed at this time (12.5 MHz) to a peak density the value obtained is about  $2 \times 10^{12}$  e1/m<sup>3</sup>, which is about a factor of 3 less than the FPS-85 measurements. In view of the quality of the Fb trace and the questionable interpretation of the critical frequencies, however, these values cannot be considered very reliable and any agreement may be fortuitous. The calculations illustrate the values one would obtain when the barium cloud is treated as a thick slab with a well defined peak electron concentration.

Ionograms for CAROLYN are shown in Figure A-8. There is no evidence of any Eb returns, but a weak, direct Fb trace can be seen at 0012 and is visible until 0024 UT between 5 and 10 MHz at a virtual height of approximately 200 km.

Similar weak F-region returns (Fb) are also evident in the DIANNE ionograms presented in Figure A-9. The echo is first seen at 0046 UT and is visible until 0114 UT at a virtual height of 200 km. Weak mixed-mode echoes are apparently present at 0024 UT.

In ESTHER a natural sporadic-E layer can be seen in the first ionogram in Figure A-10 and is visible throughout the sequence. (There is no question of the origin of this trace because this layer is present prior to the release of ESTHER at 2301 UT.) Although the cloud is definitely present at 2319 UT between 4 and 10 MHz, there is evidence of a mixed-mode echo occurring earlier at 2305 UT and also in the following two ionograms. Mixed-mode returns are also apparent in Figure A-10 at 0005 to 0012 UT.

Both E- and F-region returns from the barium cloud were observed in FERN. Unlike the Eb returns in ESTHER, the Eb returns in FERN show a clear range variation with time as would be expected from a layer

drifting toward the ionosonde and passing overhead. In addition the sequence of ionograms between 2253 and 2355 UT clearly shows that the Eb layer originated from the barium cloud. Thus, it is clear that the Eb-trace in FERN is barium-cloud-related.

The Eb-layer passed overhead at approximately 0025 UT (minimum height of 106 km) and was last seen at 0220 UT at a height of 135 km. There are hints of the Fb trace at approximately 135 km for the next 13 hours. Equally suggestive of this layer is that on occasion mixed-mode F-region returns can be seen (see ionograms at 0600, 0620, and 0740). Finally, at 1520 UT (0920 LT) a strong return can be seen at 135 km extending between 3 and 10 MHz. Although these late returns cannot be conclusively related to the barium release, we believe that the trace at 1520 UT is cloud-related.

Appendix B  
MAGNETOMETER RESULTS



## Appendix B

### MAGNETOMETER RESULTS DURING STRESS

SRI operated an EDA three-axis fluxgate magnetometer during the STRESS program to provide a real-time monitor of the geomagnetic field. This instrument, a highly reliable solid-state unit, was operated continuously for the duration of the STRESS test. The output of the instrument was recorded on strip charts that were scanned for the presence of any unusual disturbance such as a sudden magnetic commencement. None were observed.

A summary of the magnetometer data collected is presented in Figure B-1. The magnetic index represents a 3-hour average of the data. The index ranges from 0 to 10, with 0 indicating very quiet conditions and 10 very disturbed. As can be seen in the figure the STRESS releases were conducted during a relatively inactive period when the magnetic index never exceeded 5.

The occurrence of the five STRESS releases is indicated in Figure B-1. Evidently magnetic activity was most active for ESTHER and the least active for BETTY AND FERN.

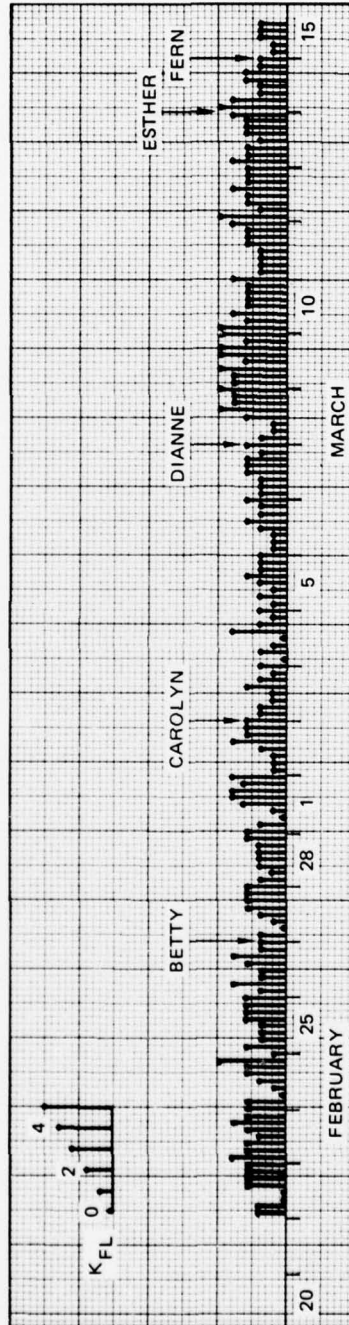


FIGURE B-1 MAGNETIC INDEX FOR EGLIN, FLORIDA DERIVED FROM EDA FLUXGATE MAGNETOMETER DURING THE STRESS PROGRAM

# DISTRIBUTION LIST

## DEPARTMENT OF DEFENSE

Director  
Command Control Technical Center  
ATTN: C-650

Director  
Defense Advanced Rsch. Proj. Agency  
ATTN: Nuclear Monitoring Research  
ATTN: Strategic Tech. Office

Defense Communication Engineer Center  
ATTN: Code R410, James W. McLean

Director  
Defense Communications Agency  
ATTN: Code 480  
ATTN: Code 810, R. M. Rostron  
ATTN: Code 101B, MAJ Hood  
ATTN: Maurey Raffensperger

Defense Communications Agency  
WWMCCS System Engineering Org.  
ATTN: R. L. Crawford

Defense Documentation Center  
Cameron Station  
12 cy ATTN: TC

Director  
Defense Nuclear Agency  
3 cy ATTN: TITL, Tech. Library  
ATTN: TISI, Archives  
ATTN: DDST  
3 cy ATTN: RAAE  
ATTN: STVL

Commander  
Field Command, DNA  
ATTN: FCPR

Director  
Joint Strat. Tgt. Planning Staff  
ATTN: JLTW-2

Chief  
Livermore Division, Fld. Command, DNA  
Lawrence Livermore Laboratory  
ATTN: FCPRL

Director  
National Security Agency  
ATTN: John Skillman, R52  
ATTN: Pat Clark, W14

Commandant  
NATO School (SHAPE)  
ATTN: U.S. Documents Officer

OJCS/J-3  
ATTN: WWMCCS, Eval. Ofc., Mr. Toma

Under Secretary of Defense for Rsch. & Engrg.  
ATTN: S&SS (OS)  
ATTN: AE

## DEPARTMENT OF THE ARMY

Director  
BMD Advanced Tech. Ctr.  
Huntsville Office  
ATTN: ATC-1

Commander  
Harry Diamond Laboratories  
ATTN: DELHD-TI, Mildred H. Weiner  
ATTN: DELHD-NP, Francis N. Wimenitz  
2 cy ATTN: DELHD-NP

Commander  
U.S. Army Nuclear & Chemical Agency  
ATTN: Library

Commander  
U.S. Army SATCOM Agency  
ATTN: Document Control

## DEPARTMENT OF THE NAVY

Chief of Naval Research  
ATTN: Code 461

Commanding Officer  
Naval Intelligence Support Ctr.  
ATTN: STIC 12, Mr. Dubbin

Commander  
Naval Ocean Systems Center  
ATTN: Code 532  
ATTN: Code 0230, C. Baggett

Director  
Naval Research Laboratory  
ATTN: Code 7730, Edgar A. McClean  
ATTN: Code 5410, John Davis  
ATTN: Code 6701, Jack D. Brown  
ATTN: Code 5430, Satellite Comm.  
ATTN: Code 6700, Timothy P. Coffey  
ATTN: Code 5400, HG. Comm. Dir., Bruce Wald

Officer-in-Charge  
Naval Surface Weapons Center  
ATTN: Code WA501, Navy Nuc. Prgms. Off.

Director  
Strategic Systems Project Office  
ATTN: Nssp-2722, Fred Wimberly  
ATTN: NSP-2141

DEPARTMENT OF THE AIR FORCE

AF Geophysics Laboratory, AFSC  
ATTN: PHD, John P. Mullen  
ATTN: OPR-1, James C. Ulwick  
ATTN: PHD, Jurgen Buchau  
ATTN: SUOL, Rsch. Lib.  
ATTN: PHP, Jules Aarons

AF Weapons Laboratory, AFSC  
ATTN: SUL  
ATTN: DYT, Capt L. Wittwer  
ATTN: DYC, John M. Kamm  
ATTN: DYM, Maj Gary Ganong

DEPARTMENT OF THE AIR FORCE (Continued)

AFTAC  
ATTN: TN

Air Force Avionics Laboratory, AFSC  
ATTN: AAD, Allen Johnson

Headquarters  
Electronic Systems Division, (AFSC)  
ATTN: Jim Deas

Commander  
Foreign Technology Division, AFSC  
ATTN: NICD Library

Commander  
Rome Air Development Center, AFSC  
ATTN: EMILD Doc. Library

SAMSO/MN  
ATTN: MNIL, Ltc Kennedy

SAMSO/SK  
ATTN: SKA, Lt Maria A. Clavin

SAMSO/YA  
ATTN: YAT, Capt L. Blackweider

Commander in Chief  
Strategic Air Command  
ATTN: XPFS, Maj Brian G. Stephan  
ATTN: ADWATE, Capt Bruce Bauer  
ATTN: NRT

DEPARTMENT OF ENERGY

University of California  
Lawrence Livermore Laboratory  
ATTN: Frederick D. Seward, L-46  
ATTN: Tech. Info. Dept. L-3

Los Alamos Scientific Laboratory  
ATTN: Doc. Con. for Robert Jefferies  
ATTN: Doc. Con. for John Wolcott  
ATTN: Doc. Con. for John Zinn

Sandia Laboratories  
ATTN: Doc. Con. for T. Wright  
ATTN: Doc. Con. for D. A. Dahlgren, Org. 1722  
ATTN: Doc. Con. for J. P. Martin, Org. 1732  
ATTN: Doc. Con. for W. D. Brown, Org. 1353

OTHER GOVERNMENT AGENCIES

Department of Commerce  
Office of Telecommunications  
Institute for Telecom Science  
ATTN: William F. Utlaut

National Oceanic & Atmospheric Admin.  
Environmental Research Laboratories  
Department of Commerce  
ATTN: C. L. Ruffnach

DEPARTMENT OF DEFENSE CONTRACTORS

Aerospace Corporation  
ATTN: T. M. Salmi  
ATTN: SMFA for PWV  
ATTN: Irving M. Garfunkel  
ATTN: Norman D. Stockwell  
ATTN: J. E. Carter, 120 Rm 2209

DEPARTMENT OF DEFENSE CONTRACTORS (Continued)

University of California at San Diego  
ATTN: IPAPS, B-019 for Henry G. Booker

COMSAT Laboratories  
ATTN: R. R. Taur

Cornell University  
Department of Electrical Engineering  
ATTN: D. T. Farley, Jr.

ESL, Inc.  
ATTN: James Marshall  
ATTN: C. W. Prettie

General Electric Company  
TEMPO-Center for Advanced Studies  
ATTN: DASIAC  
ATTN: Warren S. Knapp

General Electric Company  
ATTN: F. A. Reibert

General Research Corporation  
ATTN: Joel Garbarino  
ATTN: John Ise, Jr.

Geophysical Institute  
University of Alaska  
ATTN: Technical Library

University of Illinois  
Department of Electrical Engineering  
ATTN: K. C. Yeh

Institute for Defense Analyses  
ATTN: Ernest Bauer

Intl. Tel. & Telegraph Corporation  
ATTN: Technical Library

JAYCOR  
ATTN: S. R. Goldman

Johns Hopkins University  
Applied Physics Laboratory  
ATTN: Thomas Potemra  
ATTN: Document Librarian  
ATTN: John Dassoulas

M.I.T. Lincoln Laboratory  
ATTN: Lib. A-082 for David M. Towle

McDonnell Douglas Corporation  
ATTN: Tech. Library Services

Mission Research Corporation  
ATTN: F. Fajen  
ATTN: D. Sappenfield  
ATTN: R. Bogusch  
ATTN: Ralph Kilib  
ATTN: Dave Sowle  
ATTN: R. Hendrick

The Mitre Corporation  
ATTN: Chief Scientist, W. Sen

Physical Dynamics, Inc.  
ATTN: Joseph B. Workman

DEPARTMENT OF DEFENSE CONTRACTORS (Continued)

R & D Associates

ATTN: William J. Karzas  
ATTN: Bryan Gabbard  
ATTN: Robert E. Lelevier

The Rand Corporation

ATTN: Ed Bedrozian  
ATTN: Cullen Crain

Raytheon Company

ATTN: Barbara Adams

DEPARTMENT OF DEFENSE CONTRACTORS (Continued)

Science Applications, Inc.

ATTN: Lewis M. Linson  
ATTN: Daniel A. Hamlin  
ATTN: D. Sachs

SRI International

ATTN: Ray L. Leadabrand  
ATTN: Charles L. Rino  
ATTN: Walter G. Chesnut  
ATTN: Norman J. F. Chang

Technology International Corporation

ATTN: W. P. Boquist